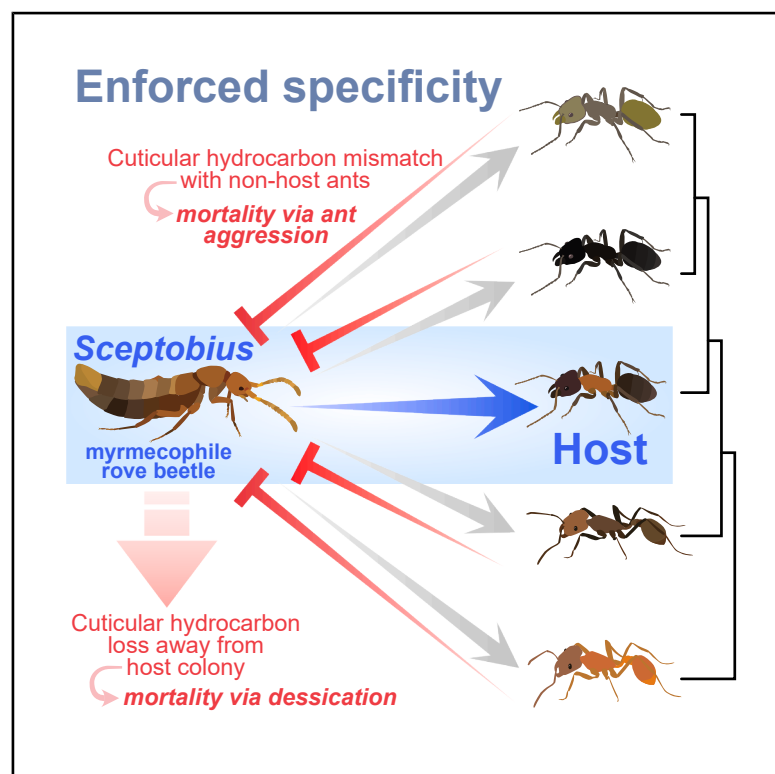


Current Biology

Enforced specificity of an entrenched symbiosis

Graphical abstract



Authors

Julian M. Wagner, Jason H. Wong, Jocelyn G. Millar, ..., Thomas H. Naragon, James Q. Boedicker, Joseph Parker

Correspondence

joep@caltech.edu

In brief

Wagner et al. uncover how the specificity of a myrmecophile rove beetle to its single host ant species arises not from sensory specialization on host cues. Instead, constraints on dispersal and aggression from non-hosts prevent the otherwise promiscuous beetle from switching to a potentially diverse spectrum of alternative ant species.

Highlights

- A myrmecophile rove beetle detects host ant pheromones to find and infiltrate nests
- The beetle lives with one ant species in nature yet accepts diverse ants as hosts
- Specificity arises not from neural preference but from constraints on switching hosts
- Enforced specificity may be typical of entrenched symbiotic lifestyles in the Metazoa

Article

Enforced specificity of an entrenched symbiosis

Julian M. Wagner,¹ Jason H. Wong,² Jocelyn G. Millar,³ Enes Haxhimali,² Adrian Brückner,¹ Thomas H. Naragon,⁴ James Q. Boedicker,² and Joseph Parker^{1,5,*}

¹Division of Biology and Biological Engineering, California Institute of Technology, Pasadena, CA 91125, USA

²Department of Physics and Astronomy, University of Southern California, Los Angeles, CA 90089, USA

³Department of Entomology, University of California, Riverside, Riverside, CA 92521, USA

⁴Division of Chemistry and Chemical Engineering, California Institute of Technology, Pasadena, CA 91125, USA

⁵Lead contact

*Correspondence: joep@caltech.edu

<https://doi.org/10.1016/j.cub.2025.10.066>

SUMMARY

The Metazoa encompasses inordinate lineages of symbionts and ecological specialists that obligately depend on particular hosts. The maintenance and fidelity of these lifestyles are often posited to hinge on sensory tuning to host-derived cues, a paradigm supported by studies of neural function in host-specific models. We experimentally reconstituted a socially complex relationship between an obligately symbiotic rove beetle and its single, natural host ant species, permitting us to probe its sensory basis. We show that cuticular hydrocarbons—the ant's nestmate recognition pheromones—elicit host recognition by the beetle and the execution of ant grooming behavior, enabling the beetle to chemically mimic its host and infiltrate the nest as a parasitic impostor. The beetle also follows host trail pheromones, permitting inter-colony dispersal. Yet the beetle also performs these symbiotic behaviors with non-host ants separated by up to ~95 million years, is able to socially assimilate into their colonies, and shows minimal sensory preference for its natural host over non-host species. Agent-based modeling reveals that the specificity of the beetle emerges not from sensory tuning but from physiological limits on dispersal and negative fitness interactions with alternative hosts, constraining the otherwise promiscuous beetle to its natural host. Recreating the *in silico* model with living insects empirically demonstrates specificity arising from these enforcing barriers. Our findings show how entrenched symbioses can obviate selection for taxonomically precise host recognition, with specificity emerging from forces external to the symbiont. Chance realization of latent compatibilities with alternative hosts may facilitate host switching, explaining the diversification and deep-time success of such taxa.

INTRODUCTION

Symbioses permeate all domains of life—the products of long-term specialization of lineages on specific hosts or partner organisms.^{1–6} Knowledge of the mechanisms that perpetuate symbiotic lifestyles is crucial to understanding their past and future evolution. A central problem is how highly specialized symbiotic taxa can persist through deep time when irreversibly enmeshed in the biology of other species and hence vulnerable to co-extinction.^{7–9} Despite the diversity of symbiotic organisms and their ecological importance, however, the phenomena that mediate lasting associations between symbionts and their focal hosts remain incompletely known.^{1,10} In the Metazoa, clades of trophic,^{11,12} mutualistic,^{5,13,14} or parasitic^{2,15–19} specialists have emerged that target highly restricted host ranges, often obligately so. Many such specialists exhibit behavioral attraction to host-derived sensory information,^{14,20–30} a phenomenon commonly invoked as a functional basis that both underpins host associations and explains their often-strict fidelity.^{11,24,31–41} Enhanced neural processing of host cues can confer adaptive value, enabling specialists to more effectively detect and exploit favorable species, while simultaneously limiting interactions with other members of the community.^{32,42–44} Neural-based models

of host specificity are supported by studies of the nervous system, where specialists display increased sensitivity to host cues in peripheral^{45–52} and central brain circuits,^{53–55} as well as greater anatomical investment in brain regions associated with host cue transduction.^{46,56–59}

Evidence for the sensory tuning paradigm comes primarily from mobile specialists, such as flight-capable insects^{36,60} and host-seeking helminths^{48,61} that contend with varying environmental stimuli to locate hosts. For such taxa, perceptual sensitivity to host cues against a non-target background is likely essential. Yet outside of this paradigm, diverse modes of symbiosis exist for which the bases of host specificity remain largely unexplored. Many lifestyles, including forms of ecto- and endoparasitism,⁶² social parasitism,^{63–66} and intimate mutualisms,^{67,68} involve taxa that live in close physical and/or behavioral engagement with specific hosts and are incapable of living apart from them. The extent to which sensory cues cement these entrenched associations is unknown. In addition to sensory information, ecological forces, including pressure from natural enemies^{69,70} and limitations on dispersal capacity or host encounter probability,^{71–74} could in principle shape the realized host range. How these and other processes contribute to patterns of host association observed in nature remains an open

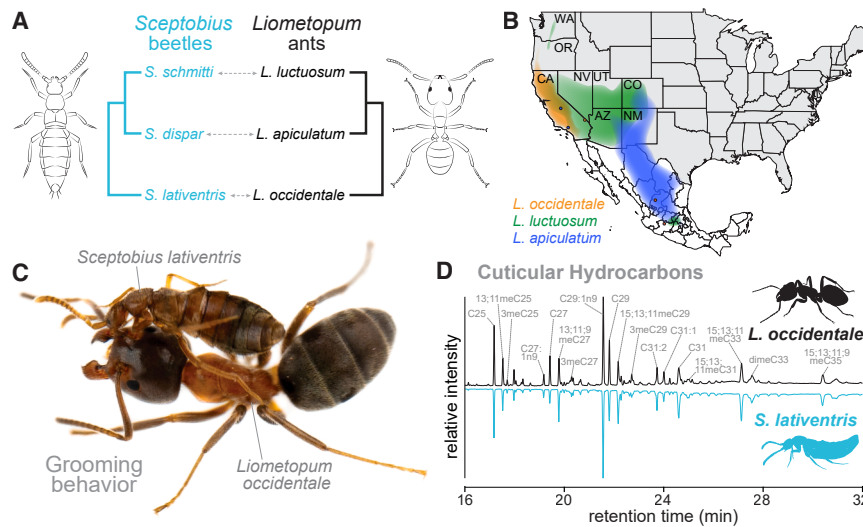


Figure 1. A model ant-mymecophile system

(A) Three *Sceptobius* species associate with different *Liometopum* hosts.
(B) Ranges of *Liometopum* species in North America, showing partial sympatry.
(C) *S. lativentris* grooming a *L. occidentale* worker.
(D) Gas chromatograph traces of *L. occidentale* ant (black) and *S. lativentris* beetle (blue, inverted), with identities of CHC peaks indicated. See also Figure S1 and Video S1.

RESULTS

The myrmecophile *Sceptobius*

Three ant species of the genus *Liometopum* (Formicidae: Dolichoderinae) are widespread in southwestern North

question, in part due to the challenges of experimentally probing complex species interactions. Adding to this problem is an evolutionary conundrum of how such taxa, which appear locked into narrow host niches, can nevertheless persist and diversify by switching to phylogenetically divergent hosts—a paradox given their extreme obligate lifestyles and host selectivity.^{10,74–77} The attributes of symbiotic systems that permit host switching are, in most cases, unknown but play a critical role in the long-term evolution of symbiont lineages.

Here, we have reconstituted a socially complex, obligate symbiotic interaction in experimental contexts that allow us to dissect the symbiont's mechanisms of host finding and host recognition and illuminate the basis of its strict specificity toward a single, natural host species. Myrmecophiles are symbionts that depend on ant societies and represent an archetype of extreme ecological specialization.⁷⁸ These diverse organisms include many phenotypically elaborate taxa that employ sophisticated strategies to infiltrate and parasitically exploit host colonies.^{64,78–81} Such relationships are often behaviorally intimate,^{79,82–94} obligate, and specific to single ant hosts.^{79,91,95–102} Rapid mortality of some myrmecophiles is observed on removal from nests.^{95,103} Despite this acute dependence, host switching is prominent across clades of myrmecophiles and has likely been key to their diversification.^{92,104–108} Herein, we harness a myrmecophile-ant system as a tractable insect model of entrenched symbiosis. We demonstrate the sensory basis of the myrmecophile's interactions with its host and show that these do not account for its specificity. When permitted, the symbiont accepts a far broader range of potential ant hosts. We instead show that external forces, operating beyond the symbiont's own agency, act to override this latent promiscuity, enforcing its specificity to a single ant host—thereby creating the illusion of host preference. These enforcing barriers are not absolute, however, resulting in scenarios where the myrmecophile can transition to novel hosts. Counter to the sensory tuning paradigm, our findings support an alternative model of host specificity and show that selection for sensory discrimination of specific hosts can be negligible in entrenched symbioses, removing a neural barrier to such organisms switching partners during evolution.

America, forming vast colonies of $\sim 10^6$ workers that forage across hundreds of square meters of habitat.¹⁰⁹ Each *Liometopum* species plays host to one of three myrmecophile species of the rove beetle genus *Sceptobius* (Staphylinidae: Aleocharinae). The beetles are hypothesized to have co-specified with *Liometopum*^{110–112} (Figure 1A), each being host specific despite partial sympatry of the three ant species (Figure 1B). Of these host-symbiont pairings, *Sceptobius lativentris* and *Liometopum occidentale* are abundant across southern California, including field sites in the Angeles National Forest. *S. lativentris* exhibits strict partner fidelity in nature, having been recorded exclusively with *L. occidentale*.¹¹¹ The beetles are tightly integrated in nests and strongly attracted to ants. When placed with a worker, *Sceptobius* climbs onto its body, clasping the ant's antenna in its mandibles (Figure 1C; Video S1). Secured to the ant in this way, the beetle repeatedly “grooms” the worker's body with its tarsi, alternating with rubbing its tarsi over its own body.¹⁰³ Grooming functions to transfer cuticular hydrocarbons (CHCs)—the ant's nestmate recognition pheromones^{113–115}—onto the beetle's cuticle. Via this interaction, the beetle achieves chemical mimicry, its CHC profile perfectly matching that of the ant, enabling it to gain social acceptance (Figure 1D).¹⁰³ Inside nests, *Sceptobius* lives as a parasitic impostor that is fed trophallactically (mouth-to-mouth) by workers and also feeds on the ants' eggs and larvae.¹⁰³

In a separate study, we have found how *Sceptobius* evolved its ability to integrate into colonies via a mechanism that silences its own, endogenous biosynthesis of CHCs.¹⁰³ In this way, the beetle achieves a chemically undetectable “stealth” phenotype, permitting it to horizontally acquire the ant's CHC profile via grooming. Crucially, CHCs create a waxy barrier on the insect body surface, which performs an essential second function in preventing desiccation.¹¹⁶ A chronic, physically close association with ants is therefore critical for *Sceptobius* survival—both to sustain its chemical mimicry and social acceptance within nests and to safeguard against physiological water loss.¹⁰³ Consequently, *Sceptobius* may spend over half of its adult life grooming ants¹¹¹ and is unable to live away from them. The beetle rapidly desiccates and dies when isolated from colonies.¹⁰³

and has evolved to be flightless.¹¹⁰ The entire life cycle takes place in close association with host colonies: adult females lay eggs in soil directly at nest entrances where they undergo imaginal development, emerging as adults that re-enter the parental colony (see [Figure S1](#) for details of *Sceptrobius* life history). Adult beetles can, however, disperse potentially long distances to new nests by navigating along actively used *L. occidentale* foraging trails, which traverse the forest floor. *Sceptrobius* is therefore deeply entrenched within the biology of a single ant species on which it is entirely dependent for survival and propagation. We asked what mechanisms perpetuate the association between this obligate symbiont and its host.

Sensory control of myrmecophile host recognition

We found that the symbiotic biology of *Sceptrobius* can be reconstituted in the laboratory. The beetle readily performs stereotyped interactions with ants in experimental contexts that have allowed us to examine their sensory basis and test their potential role in explaining the beetle's natural host specificity. We first constructed a behavioral platform to quantitatively study the beetle's grooming behavior, comprising a multiplexed array of interaction arenas assayed in the dark and illuminated with infrared light to eliminate visual stimuli ([Figures 2A, S2A, and S2B](#)). We placed single pairs of beetles and ants into arenas and trained a deep-learning neural network¹¹⁷ to follow keypoints on both insects, tracking their movement over 2 h ([Figures 2A and S2C; Video S2](#)). During trials, *Sceptrobius* climbed onto the ant, performing repeated grooming bouts that were readily classified by clustering of beetle and ant keypoints within 3 mm for at least 30 s ([Figure 2B; Video S2](#); note that prior descriptions of *Sceptrobius* behavior,¹¹¹ supported by our own observations, show that ~95% of the time that beetles are close to ants is spent mounted on or grooming them, so this simple proximity metric robustly captures the behavioral attraction represented by grooming interactions). Individual grooming bouts varied in duration, from minutes to over 1 h, with beetles usually spending over half of the total time of each trial grooming ([Figure 2G](#)).

To find the cues governing the strong physical attraction of *Sceptrobius* to its host, we substituted non-ant insects of the same approximate size and shape as *L. occidentale* into arenas with *Sceptrobius*. On introduction of a hemipteran bug (*Scolopostethus* sp.) that inhabits leaf litter near *L. occidentale* colonies,¹¹⁸ no behavioral interaction was observed ([Figures 2C and 2G; Video S2](#)), signifying that *Sceptrobius* can distinguish its host from non-ants. Identical results were obtained with other non-ant insects ([Figure 2G](#)). We hypothesized that *Sceptrobius* discriminates its host using chemosensory information on the ant body. Indeed, *Sceptrobius* is attracted to and will groom dead *L. occidentale* worker ants, demonstrating that host recognition does not require kinematic features of living ants ([Figures 2D and 2G; Video S3](#)). Conversely, when external chemical secretions are stripped from the dead ant by repeated hexane washes, grooming is lost, indicating that other features of the ant body, such as cuticle microsculpture, do not release grooming ([Figures 2E and 2G; Video S2](#)). If the ant is hexane washed to the point of strongly decreasing, but not removing, external chemical secretions, grooming still occurs ([Figure 2G](#)). We conclude that *Sceptrobius* is highly sensitive to chemicals on the ant surface that function as host recognition cues.

We determined which types of ant compound elicit grooming. Hexane extracts of crude body washes of *L. occidentale* workers contain three major compound classes: CHCs (the ant's nestmate recognition cues), 6-methyl-5-hepten-2-one (sulcatone; a volatile compound emitted as an alarm pheromone¹¹⁹), and iridoids—compounds shown to function as trail pheromones in related ant species.^{120,121} The sulcatone and iridoids are excreted by abdominal glands.¹²² Accordingly, crude hexane extracts of *L. occidentale* with gasters removed possess only CHCs, without detectable sulcatone and iridoids ([Figure S2D](#)). Nevertheless, we observe *Sceptrobius* grooming gasterless *L. occidentale* equivalently to intact ants ([Figures 2G and S2E; Video S3](#)), implying that CHCs, rather than iridoids or sulcatone, elicit ant grooming. To unequivocally confirm this, we took an unusual approach. We have found that two rove beetle genera, *Platysa* (Aleocharinae: Lomechusini) and *Liometoxenus* (Aleocharinae: Oxypodini), have, in addition to *Sceptrobius*, convergently evolved to target colonies of *L. occidentale*.¹⁰³ Both *Platysa* and *Liometoxenus* chemically mimic the CHCs of *L. occidentale*, displaying the same set of hydrocarbon compounds on their bodies in similar ratios to their host.¹⁰³ These myrmecophiles cluster closely with the ant in chemical space ([Figure 2H](#)). Importantly, unlike *Sceptrobius*, *Platysa* does not groom ants and has been found to endogenously synthesize its own CHC profile.¹⁰³ Similarly, *Liometoxenus* likely synthesizes at least some of its own CHCs as well. These beetles therefore present the same CHCs as *L. occidentale* but lack other non-CHC cues that may be present on the host ant body surface (this is especially so for *Platysa*, which only transiently interacts with workers). If *L. occidentale* CHCs are necessary and sufficient releasers of grooming behavior, *Sceptrobius* should groom these other beetles. Indeed, when placed into arenas with either of these myrmecophile rove beetles, *Sceptrobius* mounted and groomed them, much like it does *L. occidentale* ([Figures 2F and 2G; Video S3](#)). Conversely, *Sceptrobius* did not groom a free-living rove beetle, *Dalotia*¹²³ (Aleocharinae: Athetini) ([Figure 2G](#)), CHCs of which are dissimilar to those of *L. occidentale* ([Figure 2H](#)).¹²⁴ We conclude that *Sceptrobius* recognizes *L. occidentale* CHCs, which elicit grooming behavior that achieves chemical mimicry, thereby socially integrating the beetle into the colony.

Iridoid trail pheromones elicit host finding and dispersal

In addition to CHC-based host recognition, *Sceptrobius* detects additional ant compounds that tie it to its host. We observe beetles walking along networks of *L. occidentale* foraging trails in the Angeles National Forest—a behavior that permits flightless, desiccation-prone *Sceptrobius* to disperse while remaining physically close to ants. Limited aggression and significant trail connectivity exist between distant *L. occidentale* colonies,¹²⁵ likely permitting *Sceptrobius* to find new nests. We investigated the sensory basis of trail following by permitting an *L. occidentale* colony to forage through a large arena, into which we placed irregularly shaped obstacles ([Figures 3A and S3A](#)). We tracked cumulative ant density over 12 h to map a trail formed around the obstacles ([Figures 3A and S3B](#)). We removed the ants and obstacles and introduced a single worker ant into the vacant area for ~2 h ([Figures S3C and S3D](#)). The ant's movement corresponded closely to the region of highest ant density, confirming that the foraging ant colony left behind a robust chemical trail ([Figures 3B, 3E, and S3D](#)). When a *Sceptrobius* beetle was

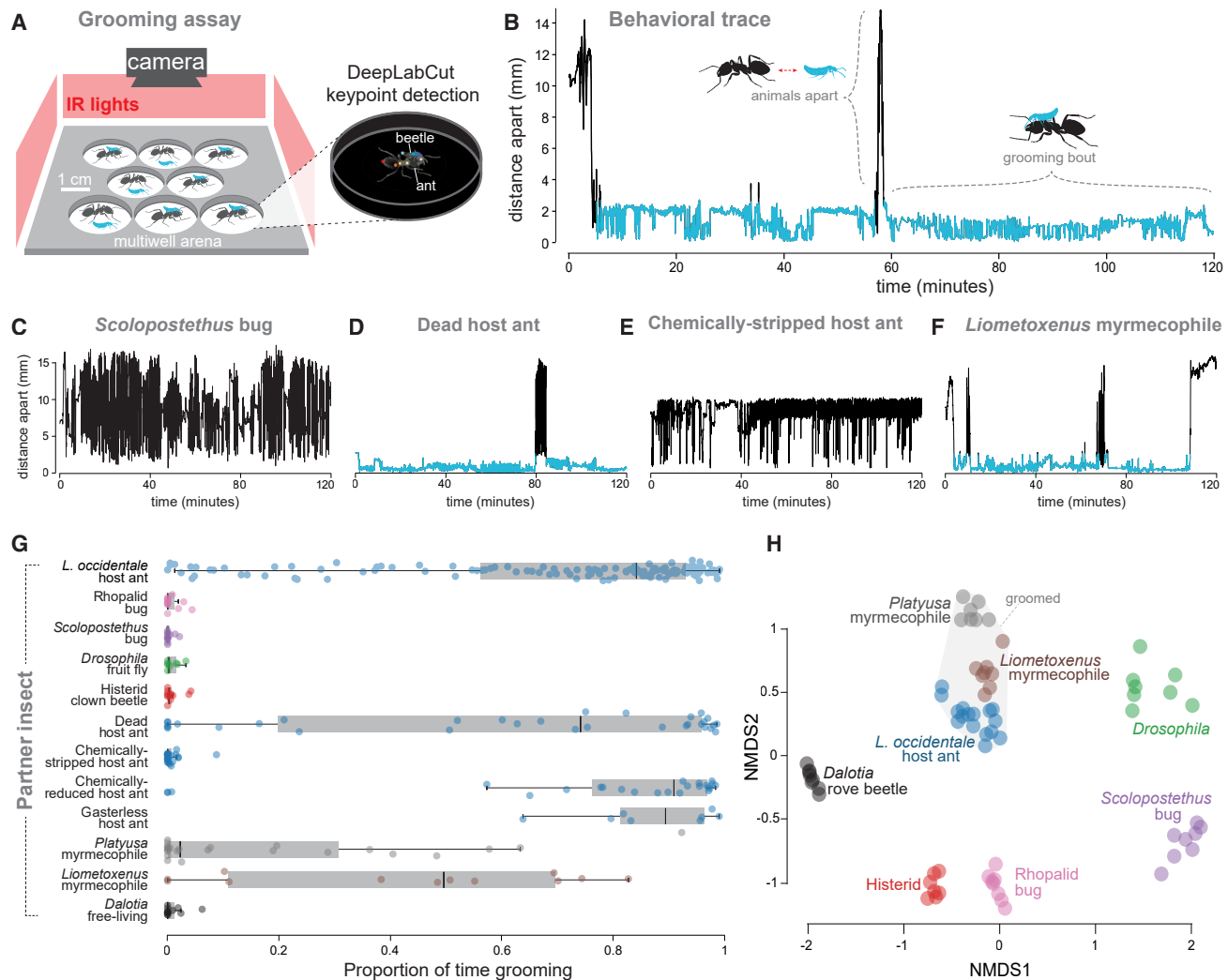


Figure 2. CHCs are host recognition cues

(A) Multi-arena behavioral platform to quantify grooming behavior.

(B) Representative 2-h behavioral trace. Blue stretches indicate grooming bouts where beetles and ants converge for ≥ 30 s, and black indicates non-grooming periods.

(C) *Sceptobius* does not groom a hemipteran bug.

(D) *Sceptobius* grooms dead *L. occidentale* worker ants.

(E) *Sceptobius* does not groom dead, chemically stripped *L. occidentale* workers.

(F) *Sceptobius* grooms other myrmecophiles that mimic *L. occidentale* CHCs.

(G) Box plot summarizing proportion of trial spent grooming during 2-h experiments.

(H) NMDS plot of CHC profiles from insect species assayed for grooming. Insects that *Sceptobius* grooms cluster closely in CHC chemical space relative to non-groomed insects (gray convex hull).

See also Figure S2 and Videos S2 and S3.

introduced into the vacant arena, its movement over 2 h also matched the shape of the *L. occidentale* trail (Figures 3C, 3E and S3E). By contrast, neither the movement of a free-living *Dalotia* rove beetle (Figure S3F) nor the movement of *Sceptobius* in an empty trail-free arena (Figures 3D and 3E) showed any correspondence with ant trail shape. These results indicate that *Sceptobius* follows chemical trails laid by its host—a behavior observed in other myrmecophile species.^{126–129}

We found that when crude ant chemical extracts are painted in a ring shape on a ground-glass arena floor, *Sceptobius* will follow

these circular trails, often for many revolutions (tens to hundreds of meters) (Figure 3F; Video S4). Exploiting this assay, we identified which *L. occidentale* compounds function as trail pheromones. Fractionating crude ant extracts, we recovered a nonpolar portion containing the full complement of CHCs and a polar fraction comprising a series of stereoisomers of two iridoids: iridodial and nepetalactol (Figure S3G). Using a multiplexed, glass-floored arena, we quantified insect movement around circular trails of CHCs or iridoids over 2 h (Figures 3F, 3G, S3H, and S3I). Both ants and *Sceptobius* exclusively followed iridoid trails, confirming

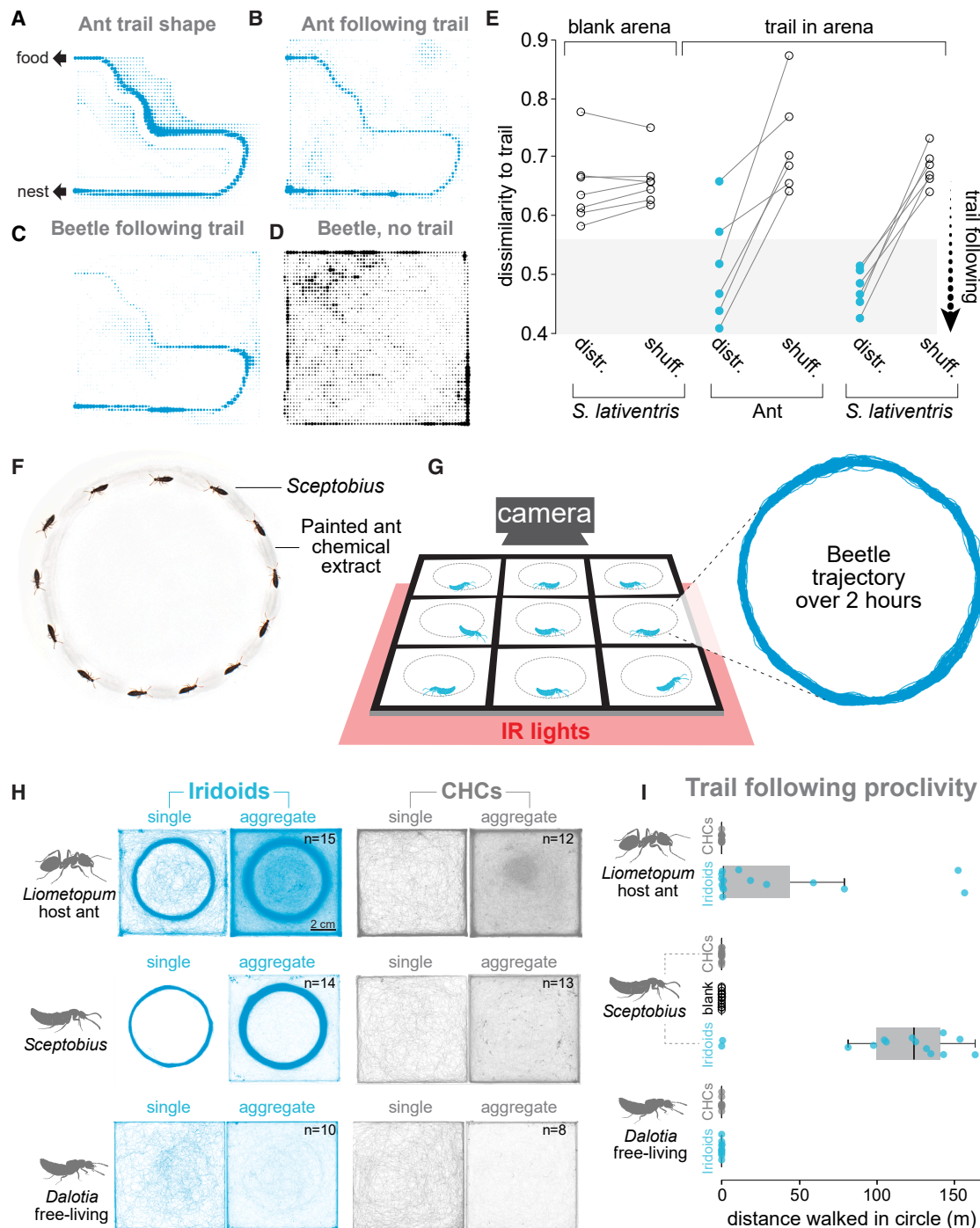


Figure 3. Iridoid trail following

(A–D) Density plots of animal movement within the foraging arena.

(A) Cumulative *L. occidentale* movement in the arena shows trail formation around obstacles.

(B and C) Movement of a single worker ant (B) or *Sceptobius* (C) in a vacant arena following removal of the colony and obstacles.

(D) *Sceptobius* walks mostly around the arena perimeter in the trail-free arena.

(E) Trail following accuracy using a dissimilarity measure derived from the Bhattacharyya coefficient. Movement of *Sceptobius* and ant corresponds closely to trail distribution (distr.); randomly shuffling beetle or ant movement traces abolishes the close match to the trail distribution (shuff.), indicating that random movement cannot account for correspondence of beetle and movement with ant trail, and beetle movement in an empty arena had an equally negligible fit to trail shape as a randomly shuffled movement trace.

(F) Timelapse composite showing *Sceptobius* following a painted ant extract circle for one revolution.

(G) Multiplexed behavioral arena to monitor trail following.

(legend continued on next page)

that these compounds are the trail pheromones (Figures 3H and 3I; Videos S5A and S5B). Again, the free-living rove beetle *Dalotia* failed to follow either CHC trails or iridoid trails, further demonstrating that trail following is a derived, symbiotic behavior of *Sceptrobius* (Figures 3H and 3I; Video S5C).

Ant chemical cues do not mediate host specificity

Our findings show that *Sceptrobius* has evolved to eavesdrop on two major components of ant communication and interprets them in a manner analogous to that of its host ant. *Sceptrobius* uses the ant's CHC nestmate recognition cues as host recognition cues and follows the ant's iridoid foraging trails for probable dispersal and host finding. Via these mechanisms, *Sceptrobius* sustains a tight, obligate association with its host. We hypothesized that these same chemicals mediate the strict association of *S. lativentris* with its single host ant species, in accordance with the sensory tuning paradigm of host specificity. We therefore tested whether *L. occidentale* chemical cues were the sole releasers of the beetle's symbiotic behaviors.

Surprisingly, despite the absolute specificity of the *S. lativentris*-*L. occidentale* association in nature, we discovered that *S. lativentris* is profoundly promiscuous in the laboratory. We observed that the beetle robustly performed grooming behavior with each of its host's sister ant species, *L. luctuosum* (95% confidence interval [CI] for median percent of trial spent grooming, from bootstrap samples: 55%–82%) and *L. apiculatum* (95% CI: 7%–32%), neither of which it has ever been found in association with (Figures 4A and 4B; Video S6). In comparison, the 95% CI for median annotated “grooming” with non-ant insects is 0%–0.2%. Pushing the promiscuity further, we tested phylogenetically divergent ants and found *Sceptrobius* would groom workers from the subfamilies Myrmicinae (*Veromessor* [95% CI: 3%–19%] and *Pogonomyrmex* [95% CI: 4%–27%]) and Formicinae (*Formica* [95% CI: 4%–21%]), which diverged from the genus *Liometopum* approximately 95–100 million years ago¹³⁰ (Figures 4A and 4C; Video S6). Remarkably, not only does the beetle recognize these non-host ants and groom them, but in each case, grooming shifts the beetle's CHC profile to match that of the non-host ant (Figure 4D). Using *L. luctuosum* as an experimental non-host ant, we quantified how grooming provides acquisition of a new host ant species' pheromonal identity. We found a time-dependent shift in the CHC profile, with complete chemical mimicry of non-hosts after 24 h (Figure 4E). Once mimicry has been achieved, we saw long-term survival of *S. lativentris* in colonies of non-host ants, which can rescue the normal, rapid mortality of beetles when removed from colonies of their natural *L. occidentale* host (Figure 4F). The beetle therefore has a latent capacity to accept alternative hosts. Moreover, its chemical mimicry strategy of horizontally acquiring ant CHCs via grooming is versatile and transferable to other ants, allowing it to socially integrate into non-host colonies.

These findings show that *Sceptrobius* can, and will, break its natural partner fidelity when presented with novel ant species with which it does not associate in nature and has likely never

encountered during its evolutionary history. We therefore asked whether, faced with a choice, *Sceptrobius* might display a preference for its host. We developed a head-to-head preference assay to quantify grooming of host versus non-host ants (Figures S4A and S4B). In a choice between single workers of *L. occidentale* and *L. luctuosum*, on average, beetles spent slightly more time grooming their host (Figure 4G); however, they still spent substantial time grooming non-hosts, often alternating grooming between the two ant species (Figures 4G and S4C; Video S7). Moreover, this slight preference disappeared when dead host and non-host ants were provided, implying that the response of the non-host ant to the beetle, rather than beetle preference for its host, may explain differences in grooming duration (Figure 4G). The beetle also showed only a minor preference for its host over a phylogenetically distant non-host (*Veromessor*) (Figures 4H and S4D; Video S7). An absolute preference for host over non-host workers therefore cannot explain the natural host specificity of *Sceptrobius*. Analysis of the CHCs from ant species groomed by *Sceptrobius* revealed an “ant cluster” in chemical space, which also encompassed the two myrmecophile beetles that *Sceptrobius* groomed and excluded all insects that *Sceptrobius* ignored (Figure 4I). We conclude that the beetle's chemosensory system is coarsely tuned to identify ants and cannot discriminate host and non-host ants. Consequently, both hosts and non-hosts are recognized as potential partners, eliciting comparable grooming behavior.

We explored whether *Sceptrobius* displays specificity for host foraging trails. We allowed field-collected workers of the sister ant species, *L. luctuosum*, to lay chemical trails in an arena before removing the ants. *L. luctuosum* trails are also composed of iridodial and nepetalactol, but in different ratios, and possibly comprising different stereoisomers (Figure S5A). As with trails laid by its host, *S. lativentris* followed naturally laid *L. luctuosum* trails (Figure S5B). We also painted crude chemical extracts of the sister ant species in circles and found that *S. lativentris* robustly followed these trails (Figure S5C). We presented the beetle with a choice by painting abutting semi-circles of *L. luctuosum* and *L. occidentale* extracts (Figures S6A and S6B). *S. lativentris* preferred its host's trail when it was at a higher concentration than extracts from the sister ant species (Figures S6C and S6D). However, when we switched the sister ant extract to a higher concentration, the preference flipped (Figures S6C and S6D), showing that trail concentration, not ant species, drives preference. The identities of the iridoids do, however, matter: *Sceptrobius* did not follow trails of another ant, *Linepithema humile*, comprising the iridoids dolichodial and iridomyrmecin¹²¹ (Figures S6E and S6F). We infer that *Sceptrobius* follows iridodial/nepetalactol trails specifically but cannot distinguish trails laid by different *Liometopum* species.

Non-hosts and spatial barriers enforce host specificity

We have demonstrated that despite its natural host specificity, *S. lativentris* has a latent promiscuity to associate with diverse non-host ants. Its symbiotic behaviors that connect it to

(H) Individual examples and aggregate trajectories of ants, *Sceptrobius*, and free-living *Dalotia* beetles in arenas with painted iridoids or CHCs. Both worker ants and *Sceptrobius* closely followed only the iridoid fraction, while *Dalotia* followed neither chemical fraction.

(I) Quantification of trail following distances during 2-h trials.

See also Figure S3 and Videos S4 and S5.

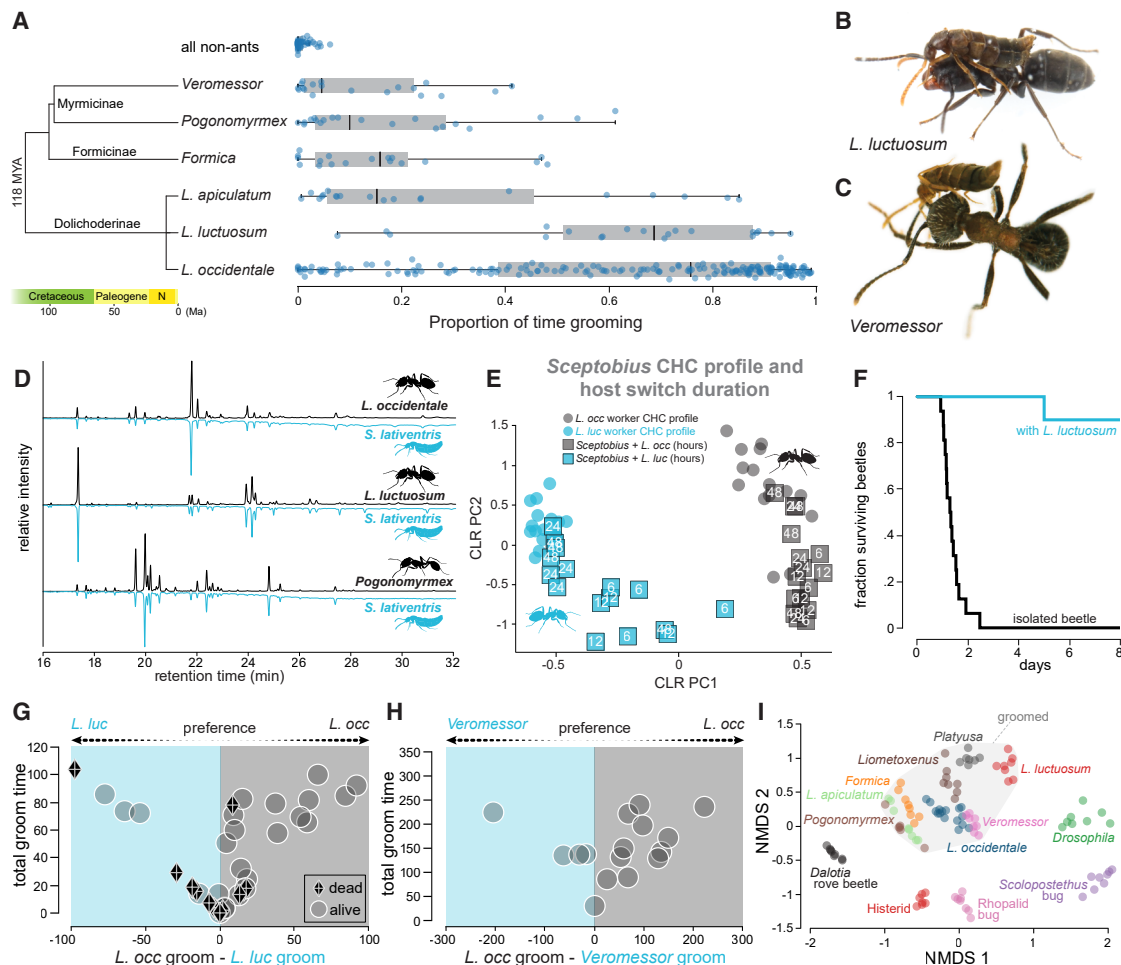


Figure 4. *Sceptobius* shows negligible chemosensory specialization on its natural host

(A) Diverse ants release *Sceptobius* grooming behavior. Dated phylogenetic tree of ants used in experiments. Box plot summarizes proportion of time spent grooming the different ant species. The proportion of time spent grooming all non-ant species is also shown for comparison.

(B and C) *Sceptobius* grooming the non-host ants *L. luctuosum* (B) and *Veromessor andrei* (C).

(D) Grooming shifts CHCs to match non-host ants.

(E) After 6–12 h of interacting, beetles are intermediate in CHC profile between the two ant species, and after 24 h match the non-host ant's profile nearly perfectly in chemical space.

(F) *Sceptobius* dies rapidly when removed from *L. occidentale* colonies (black line) but can survive inside colonies of *L. luctuosum* once integrated (blue line).

(G and H) Beetles show a weak preference for host ants in a choice assay with non-hosts *L. luctuosum* (G) and *Veromessor* (H); however, preference disappears when the beetle chooses between dead host and non-host workers (diamonds).

(I) CHC composition analysis reveals a cluster in chemical space of all the ants and groomed animals, demarcated by the gray convex hull.

See also Figures S4–S6 and Videos S6 and S7.

its host are transferable to non-hosts, and the beetle shows limited preference for its host when given a choice. The cue space that releases symbiotic behavior from *Sceptobius* therefore cannot, by itself, explain the beetle's host specificity. Additional forces must prevent the beetle's promiscuity from being realized in natural contexts, constraining its association to *L. occidentale* alone. To identify what these forces might be, we created an agent-based model,¹³¹ capturing critical aspects of *Sceptobius* biology that influence its interactions with ants. Using this model, we asked what conditions promote versus repress host switching between nests of different ant species. We then recreated our *in silico* model with living insects to experimentally test these predictions. Our model is built around three core parameters:

- (1) Intrinsic mortality. *Sceptobius* dies rapidly when isolated from ants, with heightened mortality in dry environments (Figure 5A). A major cause of death is the loss of desiccation-preventing CHCs, which isolated beetles can no longer acquire via ant grooming (Figure 5B).¹⁰³ Beetles in humid arenas are partially protected from the hazards of CHC loss but still die within ~2 days of isolation. We encoded this information in a parameter, ΔCHC_{loss} (Figure 5D). Simulated beetles lose CHCs at a specified linear rate when isolated from ants and die when CHCs are depleted. On re-encountering ants, they replenish their CHCs if they survive the interaction (Figure 5D). Wrapped into ΔCHC_{loss} are other, presently unknown,

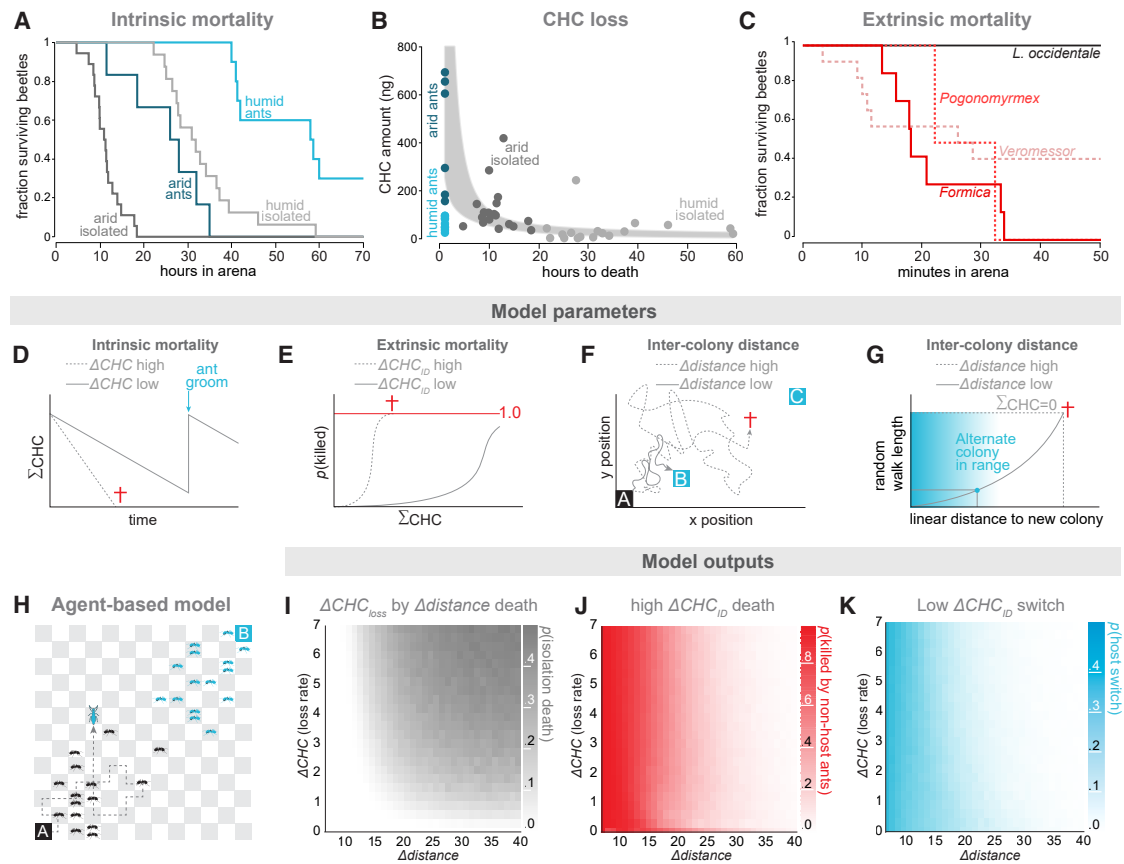


Figure 5. Constraints on host switching

- (A) Beetles rapidly die when isolated from hosts in non-humid conditions.
- (B) CHCs drop steeply on isolation from ants. Gray shaded area shows the 95% CI for a regression of exponential CHC loss calculated via non-parametric bootstrapping.
- (C) Non-host ants (red lines) quickly kill beetles when their mandibles are unimpeded.
- (D–G) Illustrations of model core parameters, and red crosses indicate beetle death.
- (D) Beetles lose CHCs at a rate of ΔCHC and regain CHCs when they groom an ant.
- (E) Probability of death in an ant encounter scales with ΔCHC_{ID} as a function of total CHCs on the beetle's body (ΣCHC).
- (F) As linear distance between ant nests increases (colony A → colony C instead of colony B), the path length for randomly walking beetles increases non-linearly.
- (G) The likelihood that the condition $\Sigma\text{CHC} = 0$ will be met scales non-linearly with path length.
- (H) Agent-based model: host and non-host ants move randomly through a discretized landscape from opposing colonies, and beetles exit the host colony and lose CHCs but can groom and regain them, die from CHC loss or ant aggression, or switch to neighboring ants of varied aggression.
- (I) The model predicts beetles die alone from desiccation as distance between ant colonies increases.
- (J) Aggressive ants kill beetles, preventing host switching.
- (K) Low-aggression ants permit host switching when colonies are close together.

See also Figure S7.

ant-dependent physiological processes that contribute to the rapid intrinsic mortality of isolated beetles.

- (2) Extrinsic mortality. Ants are innately hostile to insects with CHC profiles different from their own. *Sceptrubius* normally possesses an acquired *L. occidentale* CHC profile. Consequently, non-host ants exhibit hostility to the beetle. Indeed, to experimentally uncover *Sceptrubius*'s latent promiscuity for non-host ants (e.g., Figure 4A), it was necessary to impede the mandibles of those ants, thereby enabling *Sceptrubius* to groom them. Without doing so, non-hosts killed most beetles within 30 min (Figure 5C). Conversely, *L. luctuosum*, which possesses largely the same CHCs as *L. occidentale* but in different ratios, is

relatively less aggressive to *Sceptrubius* than the phylogenetically (and chemically) divergent non-hosts, *Veromessor*, *Pogonomymex*, and *Formica*. We encoded the degree of mismatch between host and non-host CHCs in a parameter, ΔCHC_{ID} , where a greater value increases the likelihood a non-host ant will kill *Sceptrubius* in an encounter before the beetle can acquire its CHCs (Figure 5E). The degree of aggression is modeled as a function of the total amount of CHCs (ΣCHC) on the beetle's body—higher amounts being more detectable and more likely to elicit aggression (Figure 5E).

- (3) Inter-colony distance. Ant colonies are separated by topographically complex natural terrain. We encoded linear

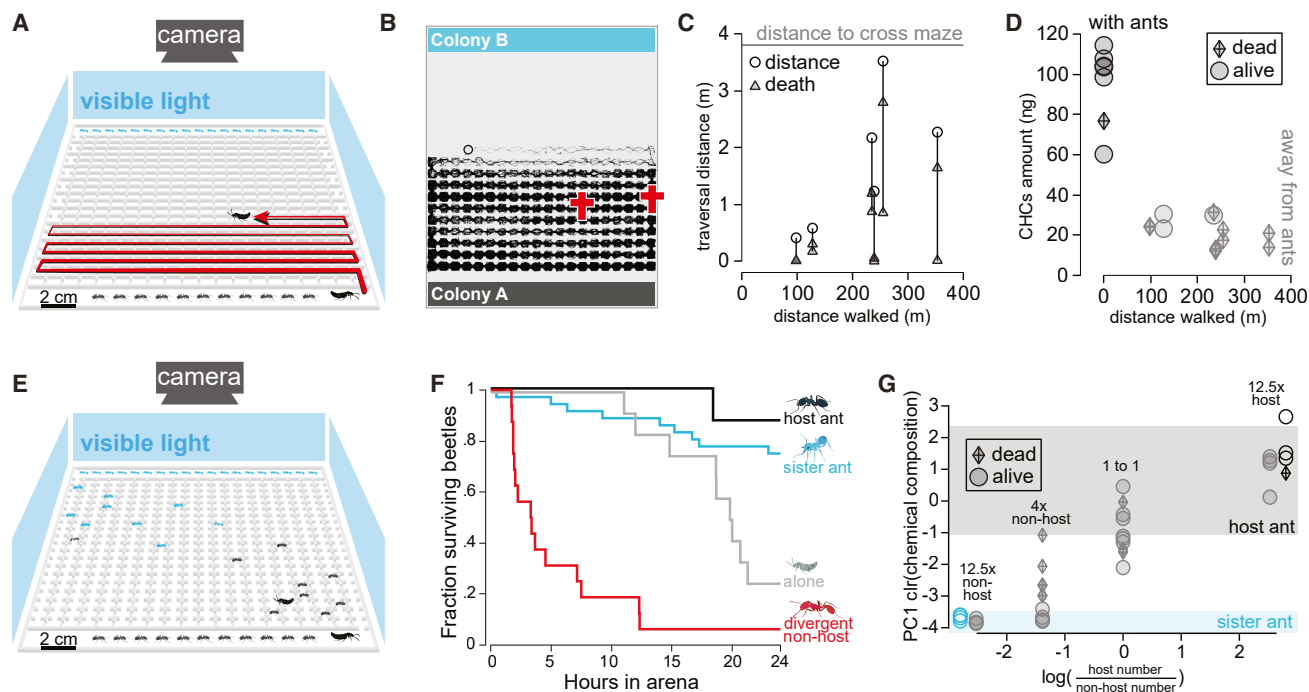


Figure 6. Experiments confirm constraints on host switching

(A) Zig-zag maze arena to test the impact of distance on moving to a new nest. Beetles can leave the host colony and enter the opposing colony, but ants are prevented from entering the arena.
(B) Traces of two beetles in the maze arena (black) show wandering but no successful arena crosses. The † symbols indicate positions at which beetles died.
(C) None of the twelve beetles successfully crossed the maze (shortest traversal path ~4 m, the farthest traversal distance reached by a beetle in a trial indicated as “distance,” and the shorter distance along the maze where beetles died/ended the trial indicated as “death”), despite wandering hundreds of meters within the arena.
(D) Beetles in the maze arena rapidly lost CHCs while wandering from ants, matching the model. Most died in less than a day away from ants.
(E) Interaction landscape to test host-switch potential to high- or low-aggression non-host ants.
(F) High-aggression ants rapidly kill beetles, whereas low-aggression sister ants do not.
(G) CHC composition analysis shows beetles gain non-host CHCs proportional to the ratio of host to non-hosts in the arena, with complete mimicry contingent on the beetle’s survival. Black and blue plotted points represent beetles placed with only host or only sister ants in the arena, with gray and blue rectangles indicating the 95th percentile in CHC space for host ants ($n = 30$) or non-host ants ($n = 25$).

See also Figure S7.

distance between nests in the parameter $\Delta distance$. As linear distance between nests increases, the path length that a randomly walking beetle takes to find a new nest in two dimensions increases non-linearly and would increase especially steeply for topographically complex three-dimensional substrates (Figures 5F and 5G).

We instantiated a virtual landscape comprising a grid of “forest floor” tiles, with spatially separated colonies of host and non-host ants (Figure 5H). *Sceptrubius* beetles dispersing from the host colony were permitted to interact with host and non-host ants following the rules defined above, losing CHCs at a rate of ΔCHC_{loss} if unable to encounter and successfully groom an ant. Extensive parameter screening identified conditions that prevent or favor beetles switching to the non-host colony. The model predicted three regimes. First, by keeping host and non-host ants chemically similar ($\Delta CHC_{ID} = 0.1$) but modulating landscape area, we find that beetles fail to host switch in large landscapes, instead dying from intrinsic mortality (ΔCHC_{loss}) when ant nests are far apart (Figure 5I). Second, when inter-colony distances are short, high aggression from chemically divergent ants prevents host switching, because the beetle still retains some

CHCs from its former (host) colony (Figure 5J). Finally, in scenarios where CHC divergence of non-hosts is small, the beetles can host switch—albeit contingent on non-host nests being spatially close enough to avert the beetle’s intrinsic mortality (Figure 5K). These three outcomes imply that host specificity could stem from forces independent of the beetle’s own sensory-driven interactions with ants. Despite coarse-grained attraction to general ant CHCs, a strict association with *L. occidentale* may nevertheless emerge from enforcing barriers in the form of dispersal constraints imposed by the environment outside of colonies (promoting intrinsic mortality away from ants) and deleterious behavioral interactions with non-host ants (should these interactions arise).

To empirically test these predictions, we built large-scale arenas to track beetles across a landscape with colonies of host and non-host ants, replicating our *in silico* model *in vivo* (Figures S7A and S7B). We first asked if beetles die when attempting to cross a navigation-cue-free space to a new nest. We introduced a zig-zag course and tracked whether beetles crossed from one *L. occidentale* colony to another, selectively preventing the ants themselves from entering the arena (Figures 6A and S7A). Even though the minimal path length to cross this maze was only ~4 m, no beetle successfully crossed despite typically wandering

>100 m (Figures 6B and 6C). Net movement of most beetles was <2 m along the course, and the majority ended up dying less than 1 m from their starting colony (Figure 6C). Total CHC levels on the bodies of these dispersing beetles decreased massively after leaving their parent colony (Figure 6D). These data confirm that even small inter-colony distances pose near-insurmountable barriers in the absence of navigational cues. The only viable way to exit *L. occidentale* nests in nature is likely via iridoid trails that are populated by ants, permitting dispersal but constraining *S. lativentris* to nests of this ant alone.

We next tested the prediction that, when in close enough spatial proximity to feasibly host a switch, ants with strongly dissimilar CHCs (high ΔCHC_{ID}) would reject beetles, thereby aggressively rather than spatially enforcing specificity. We built a second arena with a grid-like spatial structure through which both beetles and ants could move freely and interact, emerging from their source colonies located at opposite ends of the arena (Figures 6E and S7B). We performed trials with different numbers of host and non-host ants. Within hours, phylogenetically distant non-host ants with strongly divergent CHCs killed all beetles (Figure 6F). We observed similar results with three other species of CHC-divergent ants, confirming that even if the beetle reaches a non-host ant colony, its previously acquired *L. occidentale* CHC profile triggers aggression and prevents switching. By contrast, employing the chemically similar congeneric ant, *L. luctuosum*, we observed high survival rates for *S. lativentris* when permitted to interact with this sister ant species across a range of host: non-host ant ratios (Figures 6F and 6G). Even in the case of 20 host and 250 non-host ants, in which all host ants were killed by the sister ant species, every beetle survived, groomed the non-hosts, and switched to the *L. luctuosum* colony after acquiring the non-host's CHC profile (Figure 6G). Indeed, we found the higher the ratio of non-hosts to hosts, the closer the beetle's CHC profile became to that of the non-host (Figure 6G). Beetles with intermediate pheromone profiles were animals that died during the run, having failed to host switch (Figure 6G).

These findings support the model's prediction that divergence of *Sceptrobius*'s acquired CHC from non-host ants creates an aggression barrier to host switching—one that can be overcome if non-hosts are weakly chemically divergent. We noted that recently, in the San Bernardino mountains neighboring the Angeles National Forest, a case of sympatry of *L. occidentale* and *L. luctuosum* was documented.¹³² We visited this locality and collected numerous *S. lativentris* from multiple *L. occidentale* colonies, but no beetles were recovered from *L. luctuosum* nests despite their proximity within tens of meters of each other. We hypothesize that the enforcement barriers identified herein have so far prevented switching, but predict such an outcome is plausible within the sympatric range of these ant species. Importantly, our model also predicts that switching hosts to chemically divergent ant species may, in fact, be possible, though infrequent. This scenario can occur if the amount of CHC on the body of *Sceptrobius* needed for desiccation avoidance is lower than the minimum level that elicits detection by ants (Figure S7C). If this condition is met, beetles with strongly depleted CHC levels may overcome enforcement barriers—their impending mortality averted by chance interactions with a diversity of ant species.

DISCUSSION

The mechanisms that connect obligate symbionts to their hosts over generational and evolutionary timescales remain poorly understood. We have shown how ant sensory cues are exploited by a myrmecophile to achieve host recognition and dispersal, enabling it to perpetuate an entrenched dependence on colonies of its host. Surprisingly, we uncovered a pronounced lack of chemosensory preference of the myrmecophile for its natural host, manifested in its near-equivalent ability to use corresponding sets of chemical cues from alternative ant species. Hence, despite these ant compounds possessing many species-specific features,^{114,115} these features do not underlie the observed specificity of the myrmecophile toward its single ant host. Instead, we found that rapid mortality coupled with an inability to disperse to new ant nests without long-range dispersal cues spatially enforces the symbiont's host association (Figure 7A). Additionally, hostility of alternative ant species toward *Sceptrobius* when coated in its natural host's CHC profile limits its realized host range (Figure 7A). We demonstrated through simulation and subsequent experimental testing that these barriers suffice to make host switching rare and can enforce the association of the beetle to a single ant species. We cannot rule out that presently unknown host-derived cues may exist that attract *S. lativentris* to its natural host over alternative ant species (e.g., from nest material,¹³³ so far not studied by us). Nor can we be certain that *S. lativentris*'s life history is fully compatible with alternative ants (though we hypothesize compatibility with at least congeneric ants that are biologically similar to its natural host). Regardless, our results indicate that even if such impediments to host switching exist, the enforcement mechanisms we identify are a primary barrier, restricting the symbiont to a single host despite its lack of intrinsic preference.

The enforced host specificity of *Sceptrobius* contrasts with canonical models that implicate sensory tuning as the basis of host associations. As we have noted, these models have emerged primarily from studies of vagile specialists for which abundant competing stimuli necessitate sensory tuning, limiting interactions with off-target hosts (Figure 7B). Conversely, we propose that enforced specificity may be a key determinant of host ranges in forms of symbiosis where interactions with alternative hosts are rare,^{10,74} imposing far weaker selection for partner discrimination. Even for mobile specialists, however, enforcement may still play a critical role. In the case of phytophagy, for example, toxins from plant secondary chemistry^{11,135} and inadequate defense against natural enemies⁶⁹ may exert analogous restrictions on diet breadth and hence function as an early and sustaining force underlying the evolution of sensory tuning. In effect, *Sceptrobius* is a counterexample to these systems—one in which entrenched specialization on a single host evolves in the relative absence of alternative hosts (Figure 7C). This scenario obviates the need for accurate partner discrimination, a situation directly opposite to ecological contexts hypothesized to select for sensory tuning, and, as we have shown, acts to diminish the acuity of neural mechanisms that would otherwise limit the symbiont's interactions with non-hosts.

Our findings lead to a general prediction: that host-embedded symbionts that infrequently encounter non-host species may be

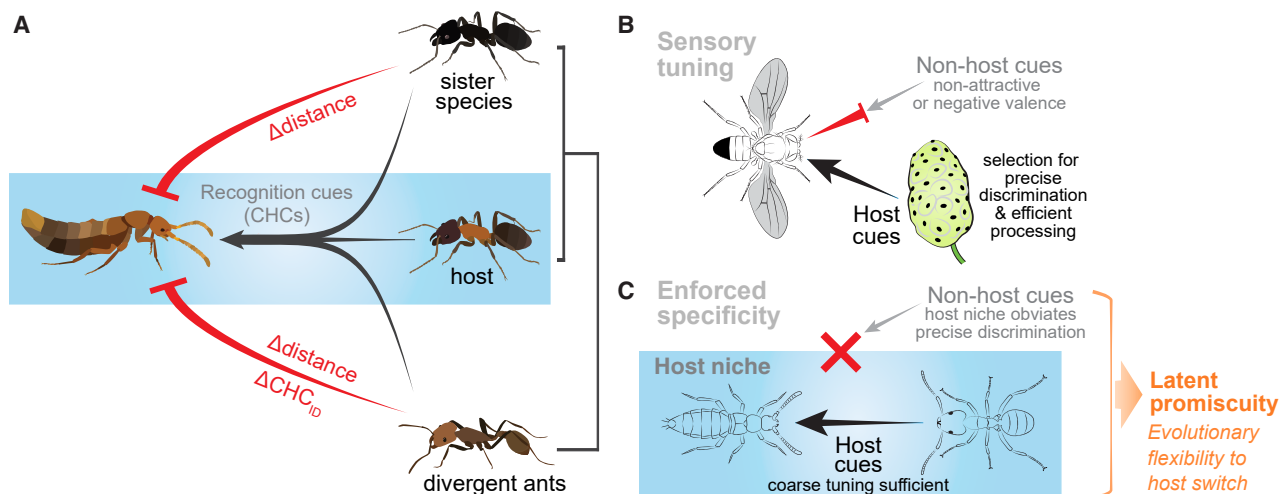


Figure 7. Forces shaping host specificity

(A) *Sceptrobius* possesses a coarse-grained ability to detect ant CHCs and enact grooming behavior, conferring a latent promiscuity to switch to other ant species. However, spatial barriers prevent switching to phylogenetically close, chemically similar ant species, and both spatial barriers and high aggression preclude switching to phylogenetically divergent, chemically dissimilar ants. (B) Sensory tuning paradigm, exemplified by *Drosophila sechellia* and its host, the noni fruit.¹³⁴ Precise tuning to host volatiles enables the mobile specialist to locate host fruit against a non-host background, conferring an intrinsic neural barrier to non-host interactions. (C) Enforced specificity, exemplified by *Sceptrobius* and its host ant. Confinement within the host colony niche removes selection for precise host discrimination, thereby weakening neural constraints on non-host interactions and conferring latent promiscuity.

those particularly predisposed to accept them as novel hosts. Ecological fitting will subsequently determine whether these nascent partnerships attain stability and lead to speciation.^{136,137} We note that many ancient lineages and speciose radiations of entrenched, host-embedded symbionts exist, persisting in the face of a high co-extinction risk. Invariably, patterns of host use across phylogenies of these taxa reveal a record of host switching,^{77,92,106,108,138–144} and evidence obtained from a variety of groups implies that their narrow host ranges may emerge, at least in part, from constraints imposed by their dispersal potential^{71,145} or the repressive actions of alternative hosts,^{84,96,146–149} paralleling the scenario we report for *Sceptrobius*. We therefore offer a further prediction: that ancient, obligately symbiotic clades may often be those that have evolved under enforced host specificity. By relaxing restraints on host recognition and acceptance, symbiotic lineages are liberated to switch to novel hosts through chance interactions, which, though rare, may ultimately be inevitable—and a catalyst for diversification.

RESOURCE AVAILABILITY

Lead contact

All correspondence and material requests should be addressed to Joseph Parker (joep@caltech.edu).

Materials availability

Materials generated for this study are available from the lead contact upon request.

Data and code availability

- Data to reproduce all figures have been deposited at CaltechData: <https://doi.org/10.22002/taxa0-k3571>.
- All original code used to generate the figures in this paper has been deposited at CaltechData: <https://doi.org/10.22002/taxa0-k3571>.
- Any additional information required to reanalyze the data reported in this paper is available from the lead contact upon request.

ACKNOWLEDGMENTS

We thank James Danoff-Burg for insights into *Sceptrobius* biology, Michael Dickinson for guidance with early behavior studies, Christiane Weirauch for bug identification, John Truong for ant husbandry, and members of the Parker laboratory for help with fieldwork. Betty Hong and Lior Pachter provided valuable input during the years of this project. This study was supported by an Army Research Office MURI grant to J.P. and J.Q.B. (W911NF1910269), with further funding to J.P. from NSF (CAREER 2047472), NIH Brain Initiative (NINDS R34NS11847), an Alfred P. Sloan Fellowship, Pew Biomedical Scholarship, Klingenstein-Simons Fellowship, and research grants from the Shurl and Kay Curci Foundation and Okawa Foundation. J.M.W. is an NSF GRFP recipient and received funding from a Rosemary Grant Advanced Award from the Society for the Study of Evolution.

AUTHOR CONTRIBUTIONS

Conceptualization, J.P., J.M.W., and J.Q.B.; data curation, J.M.W.; formal analysis, J.M.W., J.H.W., E.H., J.Q.B., and A.B.; funding acquisition, J.P., J.Q.B., and J.M.W.; investigation, J.M.W., J.H.W., E.H., A.B., T.H.N., J.G.M., and J.P.; methodology, J.M.W., J.H.W., E.H., J.Q.B., and J.P.; project administration, J.P. and J.Q.B.; resources, J.P., J.G.M., and J.Q.B.; software, J.M.W., J.H.W., E.H., and J.Q.B.; supervision, J.P. and J.Q.B.; visualization, J.P. and J.M.W.; writing – original draft, J.P. and J.M.W.; writing – review and editing, J.P., J.M.W., and J.Q.B.

DECLARATION OF INTERESTS

The authors declare no competing interests.

STAR★METHODS

Detailed methods are provided in the online version of this paper and include the following:

- KEY RESOURCES TABLE
- EXPERIMENTAL MODEL AND STUDY PARTICIPANT DETAILS
- METHOD DETAILS

- Specimen collection and husbandry of *S. lativentris* and *L. occidentale*
- Grooming behavioral arenas
- Machine learning analysis of grooming behavior
- Trail following analysis
- Identification of chemical compounds and analysis of CHC profiles
- Fractionation of ant chemical compounds
- Agent-based modeling
- Host-switching behavioral platforms
- **QUANTIFICATION AND STATISTICAL ANALYSIS**

SUPPLEMENTAL INFORMATION

Supplemental information can be found online at <https://doi.org/10.1016/j.cub.2025.10.066>.

Received: August 16, 2025

Revised: October 2, 2025

Accepted: October 22, 2025

REFERENCES

1. Poulin, R. (2007). *Evolutionary Ecology of Parasites*, Second Edition (Princeton University Press). <https://doi.org/10.1515/9781400840809>.
2. Weinstein, S.B., and Kuris, A.M. (2016). Independent origins of parasitism in Animalia. *Biol. Lett.* 12, 20160324. <https://doi.org/10.1098/rsbl.2016.0324>.
3. Casadevall, A. (2008). Evolution of intracellular pathogens. *Annu. Rev. Microbiol.* 62, 19–33. <https://doi.org/10.1146/annurev.micro.61.080706.093305>.
4. McCutcheon, J.P., Boyd, B.M., and Dale, C. (2019). The life of an insect endosymbiont from the cradle to the grave. *Curr. Biol.* 29, R485–R495. <https://doi.org/10.1016/j.cub.2019.03.032>.
5. Stadler, B., and Dixon, A.F.G. (2008). *Mutualism: Ants and Their Insect Partners* (Cambridge University Press). <https://doi.org/10.1017/CBO9780511542176>.
6. Chomicki, G., Kiers, E.T., and Renner, S.S. (2020). The evolution of mutualistic dependence. *Annu. Rev. Ecol. Evol. Syst.* 51, 409–432. <https://doi.org/10.1146/annurev-ecolsys-110218-024629>.
7. Dunn, R.R., Harris, N.C., Colwell, R.K., Koh, L.P., and Sodhi, N.S. (2009). The sixth mass coextinction: are most endangered species parasites and mutualists? *Proc. Biol. Sci.* 276, 3037–3045. <https://doi.org/10.1098/rspb.2009.0413>.
8. Colwell, R.K., Dunn, R.R., and Harris, N.C. (2012). Coextinction and persistence of dependent species in a changing world. *Annu. Rev. Ecol. Evol. Syst.* 43, 183–203. <https://doi.org/10.1146/annurev-ecolsys-110411-160304>.
9. Brodie, J.F., Aslan, C.E., Rogers, H.S., Redford, K.H., Maron, J.L., Bronstein, J.L., and Groves, C.R. (2014). Secondary extinctions of biodiversity. *Trends Ecol. Evol.* 29, 664–672. <https://doi.org/10.1016/j.tree.2014.09.012>.
10. Poulin, R., and Keeney, D.B. (2008). Host specificity under molecular and experimental scrutiny. *Trends Parasitol.* 24, 24–28. <https://doi.org/10.1016/j.pt.2007.10.002>.
11. Jaenike, J. (1990). Host specialization in phytophagous insects. *Annu. Rev. Ecol. Syst.* 21, 243–273. <https://doi.org/10.1146/annurev.es.21.110190.001331>.
12. Pineda-Munoz, S., and Alroy, J. (2014). Dietary characterization of terrestrial mammals. *Proc. R. Soc. B: Biol. Sci.* 281, 20141173. <https://doi.org/10.1098/rspb.2014.1173>.
13. Pierce, N.E., Braby, M.F., Heath, A., Lohman, D.J., Mathew, J., Rand, D.B., and Travassos, M.A. (2002). The ecology and evolution of ant association in the Lycaenidae (Lepidoptera). *Annu. Rev. Entomol.* 47, 733–771. <https://doi.org/10.1146/annurev.ento.47.091201.145257>.
14. Caves, E.M. (2021). The behavioural ecology of marine cleaning mutualisms. *Biol. Rev. Camb. Philos. Soc.* 96, 2584–2601. <https://doi.org/10.1111/brev.12770>.
15. Wiegmann, B.M., Mitter, C., and Farrell, B. (1993). Diversification of carnivorous parasitic insects: extraordinary radiation or specialized dead end? *Am. Nat.* 142, 737–754. <https://doi.org/10.1086/285570>.
16. Godfray, H.C.J. (1994). *Parasitoids: Behavioral and Evolutionary Ecology* (Princeton University Press). <https://doi.org/10.1515/9780691207025>.
17. Grimaldi, D.A. (2022). Evolutionary history of interactions among terrestrial arthropods. *Curr. Opin. Insect Sci.* 51, 100915. <https://doi.org/10.1016/j.cois.2022.100915>.
18. Pollock, H.S., Hoover, J.P., Uy, F.M.K., and Hauber, M.E. (2021). Brood parasites are a heterogeneous and functionally distinct class of natural enemies. *Trends Parasitol.* 37, 588–596. <https://doi.org/10.1016/j.pt.2021.02.005>.
19. Poulin, R., and Morand, S. (2000). The diversity of parasites. *Q. Rev. Biol.* 75, 277–293. <https://doi.org/10.1086/393500>.
20. Visser, J.H., and Avé, D.A. (1978). General green leaf volatiles in the olfactory orientation of the Colorado beetle, *Leptinotarsa decemlineata*. *Entomologia Exp. Applicata* 24, 738–749. <https://doi.org/10.1111/j.1570-7458.1978.tb02838.x>.
21. Murata, M., Miyagawa-Kohshima, K., Nakanishi, K., and Naya, Y. (1986). Characterization of compounds that induce symbiosis between sea anemone and anemone fish. *Science* 234, 585–587. <https://doi.org/10.1126/science.234.4776.585>.
22. Dickens, J.C. (1999). Predator–prey interactions: olfactory adaptations of generalist and specialist predators. *Agric. For. Entomol* 1, 47–54. <https://doi.org/10.1046/j.1461-9563.1999.00007.x>.
23. Hallem, E.A., Dillman, A.R., Hong, A.V., Zhang, Y., Yano, J.M., DeMarco, S.F., and Sternberg, P.W. (2011). A sensory code for host seeking in parasitic nematodes. *Curr. Biol.* 21, 377–383. <https://doi.org/10.1016/j.cub.2011.01.048>.
24. Wäschke, N., Meiners, T., and Rostás, M. (2013). Foraging strategies of parasitoids in complex chemical environments. In *Chemical Ecology of Insect Parasitoids*, M. Wajnberg, and S. Colazza, eds. (Wiley-Blackwell), pp. 37–63. <https://doi.org/10.1002/9781118409589.ch3>.
25. Yusuf, A.A., Crewe, R.M., and Pirk, C.W.W. (2014). Olfactory detection of prey by the termite-raiding ant *Pachycondyla analis*. *J. Insect Sci.* 14, 53. <https://doi.org/10.1093/jis/14.1.53>.
26. Mathis, K.A., and Tsutsui, N.D. (2016). Cuticular hydrocarbon cues are used for host acceptance by *Pseudacteon* spp. phorid flies that attack Azteca sericeasur ants. *J. Chem. Ecol.* 42, 286–293. <https://doi.org/10.1007/s10886-016-0694-y>.
27. Manubay, J.A., and Powell, S. (2020). Detection of prey odours underpins dietary specialization in a Neotropical top-predator: How army ants find their ant prey. *J. Anim. Ecol.* 89, 1165–1174. <https://doi.org/10.1111/1365-2656.13188>.
28. Álvarez-Ocaña, R., Shahandeh, M.P., Ray, V., Auer, T.O., Gompel, N., and Benton, R. (2023). Odor-regulated oviposition behavior in an ecological specialist. *Nat. Commun.* 14, 3041. <https://doi.org/10.1038/s41467-023-38722-z>.
29. Zhang, J., Santema, P., Lin, Z., Yang, L., Liu, M., Li, J., Deng, W., and Kempnaers, B. (2023). Experimental evidence that cuckoos choose host nests following an egg matching strategy. *Proc. Biol. Sci.* 290, 20222094. <https://doi.org/10.1098/rspb.2022.2094>.
30. Kaffle, B.D., Adesemoye, A.O., and Fadamiro, H.Y. (2024). Cuticular hydrocarbons as host recognition cues in specialist and generalist endoparasitoids. *Chemoecology* 34, 149–161. <https://doi.org/10.1007/s00049-024-00410-9>.
31. Trowbridge, C.D. (1991). Diet specialization limits herbivorous sea slug's capacity to switch among food species. *Ecology* 72, 1880–1888. <https://doi.org/10.2307/1940985>.

32. Bernays, E.A. (2001). Neural limitations in phytophagous insects: implications for diet breadth and evolution of host affiliation. *Annu. Rev. Entomol.* 46, 703–727. <https://doi.org/10.1146/annurev.ento.46.1.703>.
33. Steidle, J.L.M., and Loon, J.J.A.V. (2003). Dietary specialization and infochemical use in carnivorous arthropods: testing a concept. *Entomol. Exp. Appl.* 108, 133–148. <https://doi.org/10.1046/j.1570-7458.2003.00080.x>.
34. Bruce, T.J.A., Wadhams, L.J., and Woodcock, C.M. (2005). Insect host location: a volatile situation. *Trends Plant Sci.* 10, 269–274. <https://doi.org/10.1016/j.tplants.2005.04.003>.
35. Bruce, T.J.A., and Pickett, J.A. (2011). Perception of plant volatile blends by herbivorous insects – Finding the right mix. *Phytochemistry* 72, 1605–1611. <https://doi.org/10.1016/j.phytochem.2011.04.011>.
36. Carrasco, D., Larsson, M.C., and Anderson, P. (2015). Insect host plant selection in complex environments. *Curr. Opin. Insect Sci.* 8, 1–7. <https://doi.org/10.1016/j.cois.2015.01.014>.
37. Couto, A., Wainwright, J.B., Morris, B.J., and Montgomery, S.H. (2020). Linking ecological specialisation to adaptations in butterfly brains and sensory systems. *Curr. Opin. Insect Sci.* 42, 55–60. <https://doi.org/10.1016/j.cois.2020.09.002>.
38. Zhao, Z., and McBride, C.S. (2020). Evolution of olfactory circuits in insects. *J. Comp. Physiol. A Neuroethol. Sens. Neural Behav. Physiol.* 206, 353–367. <https://doi.org/10.1007/s00359-020-01399-6>.
39. Jones, L.C., Rafter, M.A., and Walter, G.H. (2022). Host interaction mechanisms in herbivorous insects – life cycles, host specialization and speciation. *Biol. J. Linn. Soc.* 137, 1–14. <https://doi.org/10.1093/biolinnean/blac070>.
40. Lin, P.-A., Chan, W.-P., Cai, L., Hsiao, Y., Dankowicz, E., Gilbert, K.J., Pierce, N.E., and Felton, G. (2025). The salient aroma hypothesis: host plant specialization is linked with plant volatile availability in Lepidoptera. *Proc. Biol. Sci.* 292, 20242426. <https://doi.org/10.1098/rspb.2024.2426>.
41. Attwood, M.C. (2025). How do parasites and predators choose their victim? A trade-off between quality and vulnerability across antagonistic interactions. *Biol. Rev. Camb. Philos. Soc.* 100, 2099–2115. <https://doi.org/10.1111/brv.70037>.
42. Bernays, E.A., and Wcislo, W.T. (1994). Sensory capabilities, information processing, and resource specialization. *Q. Rev. Biol.* 69, 187–204. <https://doi.org/10.1086/418539>.
43. Bernays, E.A. (1998). The value of being a resource specialist: behavioral support for a neural hypothesis. *Am. Nat.* 151, 451–464. <https://doi.org/10.1086/286132>.
44. Tosh, C.R., Krause, J., and Ruxton, G.D. (2009). Theoretical predictions strongly support decision accuracy as a major driver of ecological specialization. *Proc. Natl. Acad. Sci. USA* 106, 5698–5702. <https://doi.org/10.1073/pnas.0807247106>.
45. Matsuo, T., Sugaya, S., Yasukawa, J., Aigaki, T., and Fuyama, Y. (2007). Odorant-binding proteins OBP57d and OBP57e affect taste perception and host-plant preference in *Drosophila sechellia*. *PLoS Biol.* 5, e118–12. <https://doi.org/10.1371/journal.pbio.0050118>.
46. Dekker, T., Ibba, I., Siju, K.P., Stensmyr, M.C., and Hansson, B.S. (2006). Olfactory shifts parallel superspecialism for toxic fruit in *Drosophila melanogaster* sibling, *D. sechellia*. *Curr. Biol.* 16, 101–109. <https://doi.org/10.1016/j.cub.2005.11.075>.
47. Hansson, B.S., and Stensmyr, M.C. (2011). Evolution of insect olfaction. *Neuron* 72, 698–711. <https://doi.org/10.1016/j.neuron.2011.11.003>.
48. Gang, S.S., and Hallem, E.A. (2016). Mechanisms of host seeking by parasitic nematodes. *Mol. Biochem. Parasitol.* 208, 23–32. <https://doi.org/10.1016/j.molbiopara.2016.05.007>.
49. McBride, C.S., Baier, F., Omondi, A.B., Spitzer, S.A., Lutomiah, J., Sang, R., Ignell, R., and Vosshall, L.B. (2014). Evolution of mosquito preference for humans linked to an odorant receptor. *Nature* 515, 222–227. <https://doi.org/10.1038/nature13964>.
50. Goldman-Huertas, B., Mitchell, R.F., Lapoint, R.T., Faucher, C.P., Hildebrand, J.G., and Whiteman, N.K. (2015). Evolution of herbivory in Drosophilidae linked to loss of behaviors, antennal responses, odorant receptors, and ancestral diet. *Proc. Natl. Acad. Sci. USA* 112, 3026–3031. <https://doi.org/10.1073/pnas.1424656112>.
51. Brand, P., Hinojosa-Díaz, I.A., Ayala, R., Daigle, M., Yurrita Obiols, C.L.Y., Eltz, T., and Ramírez, S.R. (2020). The evolution of sexual signaling is linked to odorant receptor tuning in perfume-collecting orchid bees. *Nat. Commun.* 11, 244. <https://doi.org/10.1038/s41467-019-14162-6>.
52. Matsunaga, T., Reisenman, C.E., Goldman-Huertas, B., Brand, P., Miao, K., Suzuki, H.C., Verster, K.I., Ramírez, S.R., and Whiteman, N.K. (2022). Evolution of olfactory receptors tuned to mustard oils in herbivorous Drosophilidae. *Mol. Biol. Evol.* 39, msab362. <https://doi.org/10.1093/molbev/msab362>.
53. Burger, H., Ayasse, M., Dötterl, S., Kreissl, S., and Galizia, C.G. (2013). Perception of floral volatiles involved in host-plant finding behaviour: comparison of a bee specialist and generalist. *J. Comp. Physiol. A Neuroethol. Sens. Neural Behav. Physiol.* 199, 751–761. <https://doi.org/10.1007/s00359-013-0835-5>.
54. Auer, T.O., Khallaf, M.A., Silbering, A.F., Zappia, G., Ellis, K., Álvarez-Ocaña, R., Arguello, J.R., Hansson, B.S., Jefferis, G.S.X.E., Caron, S.J.C., et al. (2020). Olfactory receptor and circuit evolution promote host specialisation. *Nature* 579, 402–408. <https://doi.org/10.1038/s41586-020-2073-7>.
55. Zhao, Z., Zung, J.L., Hinze, A., Kriete, A.L., Iqbal, A., Younger, M.A., Matthews, B.J., Merhof, D., Thiberge, S., Ignell, R., et al. (2022). Mosquito brains encode unique features of human odour to drive host seeking. *Nature* 605, 706–712. <https://doi.org/10.1038/s41586-022-04675-4>.
56. Sulger, E., McAloon, N., Bulova, S.J., Sapp, J., and O'Donnell, S. (2014). Evidence for adaptive brain tissue reduction in obligate social parasites (*Polyergus mexicanus*) relative to their hosts (*Formica fusca*). *Biol. J. Linn. Soc.* 113, 415–422. <https://doi.org/10.1111/bij.12375>.
57. Montgomery, S.H., and Merrill, R.M. (2017). Divergence in brain composition during the early stages of ecological specialization in *Heliconius* butterflies. *J. Evol. Biol.* 30, 571–582. <https://doi.org/10.1111/jeb.13027>.
58. Keeseey, I.W., Grabe, V., Knaden, M., and Hansson, B.S. (2020). Divergent sensory investment mirrors potential speciation via niche partitioning across *Drosophila*. *eLife* 9, e57008. <https://doi.org/10.7554/eLife.57008>.
59. Wainwright, J.B., and Montgomery, S.H. (2022). Neuroanatomical shifts mirror patterns of ecological divergence in three diverse clades of mimetic butterflies. *Evolution* 76, 1806–1820. <https://doi.org/10.1111/evo.14547>.
60. Coutinho-Abreu, I.V., Riffell, J.A., and Akbari, O.S. (2022). Human attractive cues and mosquito host-seeking behavior. *Trends Parasitol.* 38, 246–264. <https://doi.org/10.1016/j.pt.2021.09.012>.
61. Haas, W. (2003). Parasitic worms: strategies of host finding, recognition and invasion. *Zoology (Jena)* 106, 349–364. <https://doi.org/10.1078/0944-2006-00125>.
62. Combes, C. (2001). *Parasitism: The Ecology and Evolution of Intimate Interactions* (University of Chicago Press).
63. Hölldobler, B., and Wilson, E.O. (1990). *The Ants* (Harvard University Press).
64. Kistner, D.H. (1982). The social insects' bestiary. In *Social Insects*, H.R. Hermann, ed. (Elsevier), pp. 1–244. <https://doi.org/10.1016/B978-0-12-342203-3.50008-4>.
65. Kilner, R.M., and Langmore, N.E. (2011). Cuckoos versus hosts in insects and birds: adaptations, counter-adaptations and outcomes. *Biol. Rev. Camb. Philos. Soc.* 86, 836–852. <https://doi.org/10.1111/j.1469-185X.2010.00173.x>.
66. Rabeling, C. (2020). Social parasitism. In *Encyclopedia of Social Insects*, C.K. Starr, ed. (Springer International Publishing), pp. 1–23. https://doi.org/10.1007/978-3-319-90306-4_175-1.

67. Ivens, A.B.F., and Kronauer, D.J.C. (2022). Aphid-farming ants. *Curr. Biol.* 32, R813–R817. <https://doi.org/10.1016/j.cub.2022.06.072>.
68. Geisler, L., Solodovnikov, A., and Jenkins Shaw, J.J. (2025). Oxpeckers of the mouse world: assembly and review of data on the unique mutualism between Amblyopinina rove beetles and their mammal hosts. *J. Nat. Hist.* 59, 1699–1713. <https://doi.org/10.1080/00222933.2025.2498048>.
69. Bernays, E., and Graham, M. (1988). On the evolution of host specificity in phytophagous arthropods. *Ecology* 69, 886–892. <https://doi.org/10.2307/1941237>.
70. Bernays, E.A. (1997). Feeding by lepidopteran larvae is dangerous. *Ecol. Entomol.* 22, 121–123. <https://doi.org/10.1046/j.1365-2311.1997.00042.x>.
71. Harbison, C.W., and Clayton, D.H. (2011). Community interactions govern host-switching with implications for host–parasite coevolutionary history. *Proc. Natl. Acad. Sci. USA* 108, 9525–9529. <https://doi.org/10.1073/pnas.1102129108>.
72. Bartlow, A.W., Villa, S.M., Thompson, M.W., and Bush, S.E. (2016). Walk or ride? Phoretic behaviour of amblyceran and ischnoceran lice. *Int. J. Parasitol.* 46, 221–227. <https://doi.org/10.1016/j.ijpara.2016.01.003>.
73. Doña, J., Osuna-Mascaró, C., Johnson, K.P., Serrano, D., Aymí, R., and Jovani, R. (2019). Persistence of single species of symbionts across multiple closely-related host species. *Sci. Rep.* 9, 17442. <https://doi.org/10.1038/s41598-019-54015-2>.
74. Mestre, A., Poulin, R., and Hortal, J. (2020). A niche perspective on the range expansion of symbionts. *Biol. Rev. Camb. Philos. Soc.* 95, 491–516. <https://doi.org/10.1111/brv.12574>.
75. Hoberg, E.P., and Brooks, D.R. (2008). A macroevolutionary mosaic: episodic host-switching, geographical colonization and diversification in complex host–parasite systems. *J. Biogeogr.* 35, 1533–1550. <https://doi.org/10.1111/j.1365-2699.2008.01951.x>.
76. Agosta, S.J., Janz, N., and Brooks, D.R. (2010). How specialists can be generalists: resolving the “parasite paradox” and implications for emerging infectious disease. *Zoöl. (Curitiba)* 27, 151–162. <https://doi.org/10.1590/S1984-46702010000200001>.
77. Doña, J., Sweet, A.D., Johnson, K.P., Serrano, D., Mironov, S., and Jovani, R. (2017). Cophylogenetic analyses reveal extensive host-shift speciation in a highly specialized and host-specific symbiont system. *Mol. Phylogenet. Evol.* 115, 190–196. <https://doi.org/10.1016/j.ympev.2017.08.005>.
78. Hölldobler, B., and Kwapich, C.L. (2022). *The Guests of Ants* (Harvard University Press).
79. Kistner, D.H. (1979). Social and evolutionary significance of social insect symbionts. In *Social Insects*, 1, H.R. Hermann, ed. (Elsevier), pp. 339–413. <https://doi.org/10.1016/B978-0-12-342201-9.50015-X>.
80. Parker, J. (2016). Myrmecophily in beetles (Coleoptera): evolutionary patterns and biological mechanisms. *Myrmecol. News* 22, 65–108. https://doi.org/10.25849/myrmecol.news_022:065.
81. Naragon, T.H., Wagner, J.M., and Parker, J. (2022). Parallel evolutionary paths of rove beetle myrmecophiles: replaying a deep-time tape of life. *Curr. Opin. Insect Sci.* 51, 100903. <https://doi.org/10.1016/j.cois.2022.100903>.
82. Akre, R.D. (1968). The behavior of *Euxenister* and *Pulvinister*, histerid beetles associated with army ants (Coleoptera: Histeridae; Hymenoptera: Formicidae: Dorylinae). *Pan-Pacific Entomol.* 44, 87–101.
83. Akre, R.D., and Torgerson, R.L. (1968). The behavior of *Diploeciton nevermanni*, a staphylinid beetle associated with army ants. *Psyche J. Entomol.* 75, 211–215. <https://doi.org/10.1155/1968/23814>.
84. Hölldobler, B. (1970). Zur Physiologie der Gast-Wirt-Beziehungen (Myrmecophilie) bei Ameisen. II. Das Gastverhältnis des imaginalen *Atemeles pubicollis* Bris. (Col. Staphylinidae) zu *Myrmica*, und *Formica* (Hym. Formicidae). *Z. Vgl. Physiol.* 66, 215–250. <https://doi.org/10.1007/bf00297780>.
85. Akre, R.D., and Hill, W.B. (1973). Behavior of *Adranes taylori*, a myrmecophilous beetle associated with *Lasius sitkaensis* in the Pacific Northwest (Coleoptera: Pselaphidae; Hymenoptera: Formicidae). *J. Kans. Entomol. Soc.* 46, 526–536.
86. Kistner, D.H., and Jacobson, H.R. (1990). Cladistic analysis and taxonomic revision of the ecitophilous tribe Ecitocharini with studies of their behaviour and evolution (Coleoptera, Staphylinidae, Aleocharinae). *Sociobiology* 17, 333–480.
87. Jacobson, H.R., and Kistner, D.H. (1991). Cladistic study, taxonomic restructuring, and revision of the myrmecophilous tribe Leptanillophilini with comments on its evolution and host relationships (Coleoptera: Staphylinidae; Hymenoptera: Formicidae). *Sociobiology* 18, 1–150.
88. Jacobson, H.R., and Kistner, D.H. (1992). Cladistic study, taxonomic restructuring, and revision of the myrmecophilous tribe Crematoxenini with comments on its evolution and host relationships (Coleoptera, Staphylinidae, Hymenoptera, Formicidae). *Sociobiology* 20, 91–198.
89. Kistner, D.H. (1993). Cladistic analysis, taxonomic restructuring and revision of the Old World genera formerly classified as Dorylomimini with comments on their evolution and behavior (Coleoptera: Staphylinidae). *Sociobiology* 22, 147–383.
90. Maruyama, M., Akino, T., Hashim, R., and Komatsu, T. (2009). Behavior and cuticular hydrocarbons of myrmecophilous insects (Coleoptera: Staphylinidae; Diptera: Phoridae; Thysanura) associated with Asian *Aenictus* army ants (Hymenoptera; Formicidae). *Sociobiology* 54, 19–35.
91. Komatsu, T., Maruyama, M., and Itino, T. (2009). Behavioral differences between two ant cricket species in Nansei Islands: host-specialist versus host-generalist. *Insectes Soc.* 56, 389–396. <https://doi.org/10.1007/s00040-009-0036-y>.
92. Parker, J., and Grimaldi, D.A. (2014). Specialized myrmecophily at the ecological dawn of modern ants. *Curr. Biol.* 24, 2428–2434. <https://doi.org/10.1016/j.cub.2014.08.068>.
93. von Beeren, C., Brückner, A., Maruyama, M., Burke, G., Wieschollek, J., and Kronauer, D.J.C. (2018). Chemical and behavioral integration of army ant-associated rove beetles - a comparison between specialists and generalists. *Front. Zool.* 15, 8. <https://doi.org/10.1186/s12983-018-0249-x>.
94. Hölldobler, B., and Kwapich, C.L. (2019). Behavior and exocrine glands in the myrmecophilous beetle *Dinarda dentata* (Gravenhorst, 1806) (Coleoptera: Staphylinidae: Aleocharinae). *PLOS One* 14, e0210524. <https://doi.org/10.1371/journal.pone.0210524>.
95. Akre, R.D., and Rettenmeyer, C.W. (1966). Behavior of staphylinidae associated with army ants (Formicidae: Ecitonini). *J. Kans. Entomol. Soc.* 39, 745–782.
96. Elmes, G.W., Barr, B., Thomas, J.A., and Clarke, R.T. (1999). Extreme host specificity by *Microdon mutabilis* (Diptera: Syrphidae), a social parasite of ants. *Proc. R. Soc. Lond. B* 266, 447–453. <https://doi.org/10.1098/rspb.1999.0658>.
97. Thomas, J.A., Elmes, G.W., Wardlaw, J.C., and Woyciechowski, M. (1989). Host specificity among Maculinea butterflies in *Myrmica* ant nests. *Oecologia* 79, 452–457. <https://doi.org/10.1007/BF00378660>.
98. Nash, D.R., Als, T.D., Maile, R., Jones, G.R., and Boomsma, J.J. (2008). A mosaic of chemical coevolution in a large blue butterfly. *Science* 319, 88–90. <https://doi.org/10.1126/science.1149180>.
99. Maruyama, M., Matsumoto, T., and Itioka, T. (2011). Rove beetles (Coleoptera: Staphylinidae) associated with *Aenictus laeviceps* (Hymenoptera: Formicidae) in Sarawak, Malaysia: Strict host specificity, and first myrmecoid Aleocharini. *Zootaxa* 3102, 1–26. <https://doi.org/10.11646/zootaxa.3102.1.1>.
100. von Beeren, C., Maruyama, M., and Kronauer, D.J.C. (2016). Cryptic diversity, high host specificity and reproductive synchronization in army ant-associated Vatesus beetles. *Mol. Ecol.* 25, 990–1005. <https://doi.org/10.1111/mec.13500>.

101. Maruyama, M., and Parker, J. (2017). Deep-time convergence in rove beetle symbionts of army ants. *Curr. Biol.* 27, 920–926. <https://doi.org/10.1016/j.cub.2017.02.030>.
102. von Beeren, C., Blüthgen, N., Hoenle, P.O., Pohl, S., Brückner, A., Tishechkin, A.K., Maruyama, M., Brown, B.V., Hash, J.M., Hall, W.E., et al. (2021). A remarkable legion of guests: Diversity and host specificity of army ant symbionts. *Mol. Ecol.* 30, 5229–5246. <https://doi.org/10.1111/mec.16101>.
103. Naragon, T.H., Viliunas, J.W., Yousefalahiyeh, M., Brückner, A., Wagner, J.M., Ryon, H.M., Collinson, D., Kitchen, S.A., Wijker, R.S., Sessions, A.L., et al. (2025). Symbiotic entrenchment through ecological Catch-22. Preprint at bioRxiv. <https://doi.org/10.1101/2025.07.02.662832>.
104. Fiedler, K. (2012). The host genera of ant-parasitic Lycaenidae butterflies: a review. *Psyche: A Journal of Entomology* 2012, 1–10. <https://doi.org/10.1155/2012/153975>.
105. Murray, E.A., Carmichael, A.E., and Heraty, J.M. (2013). Ancient host shifts followed by host conservatism in a group of ant parasitoids. *Proc. Biol. Sci.* 280, 20130495. <https://doi.org/10.1098/rspb.2013.0495>.
106. Moore, W., and Robertson, J.A. (2014). Explosive adaptive radiation and extreme phenotypic diversity within ant-nest beetles. *Curr. Biol.* 24, 2435–2439. <https://doi.org/10.1016/j.cub.2014.09.022>.
107. Zhou, Y.-L., Ślipiński, A., Ren, D., and Parker, J. (2019). A Mesozoic clown beetle myrmecophile (Coleoptera: Histeridae). *eLife* 8, e44985. <https://doi.org/10.7554/eLife.44985>.
108. Hlaváč, P., Parker, J., Maruyama, M., and Fikáček, M. (2021). Diversification of myrmecophilous Clavigeritae beetles (Coleoptera: Staphylinidae: Pselaphinae) and their radiation in New Caledonia. *Syst. Entomol.* 46, 422–452. <https://doi.org/10.1111/syen.12469>.
109. Hoey-Chamberlain, R., Rust, M.K., and Klotz, J.H. (2013). A review of the biology, ecology and behavior of velvety tree ants of North America. *Sociobiology* 60, 1–10. <https://doi.org/10.13102/sociobiology.v60i1.1-10>.
110. Danoff-Burg, J.A. (1994). Evolving under myrmecophily: a cladistic revision of the symphiliid beetle tribe Sceptobiini (Coleoptera: Staphylinidae: Aleocharinae). *Syst. Entomol.* 19, 25–45. <https://doi.org/10.1111/j.1365-3113.1994.tb00577.x>.
111. Danoff-Burg, J.A. (1996). An ethogram of the ant-guest beetle tribe Sceptobiini (Coleoptera: Staphylinidae: Formicidae). *Sociobiology* 27, 287–328.
112. Danoff-Burg, J.A. (2002). Evolutionary lability and phylogenetic utility of behavior in a group of ant-guest staphylinidae beetles. *Ann. Entomol. Soc. Am.* 95, 143–155. [https://doi.org/10.1603/0013-8746\(2002\)095\[0143:ELAPUO\]2.0.CO;2](https://doi.org/10.1603/0013-8746(2002)095[0143:ELAPUO]2.0.CO;2).
113. Blomquist, G.J., and Bagnères, A.-G. (2010). *Insect Hydrocarbons*, G.J. Blomquist, and A.-G. Bagnères, eds. (Cambridge University Press).
114. Sturgis, S.J., and Gordon, D.M. (2012). Nestmate recognition in ants (Hymenoptera: Formicidae): a review. *Myrmecological News* 16, 101–110. https://doi.org/10.25849/myrmecol.news_016:101.
115. Sprenger, P.P., and Menzel, F. (2020). Cuticular hydrocarbons in ants (Hymenoptera: Formicidae) and other insects: how and why they differ among individuals, colonies, and species. *Myrmecological News* 30, 1–26. https://doi.org/10.25849/myrmecol.news_030:001.
116. Gibbs, A.G., and Rajpurohit, S. (2010). Cuticular lipids and water balance. In *Insect Hydrocarbons*, G.J. Blomquist, and A.-G. Bagnères, eds. (Cambridge University Press), pp. 100–120. <https://doi.org/10.1017/CBO9780511711909.007>.
117. Mathis, A., Mamidanna, P., Cury, K.M., Abe, T., Murthy, V.N., Mathis, M.W., and Bethge, M. (2018). DeepLabCut: markerless pose estimation of user-defined body parts with deep learning. *Nat. Neurosci.* 21, 1281–1289. <https://doi.org/10.1038/s41593-018-0209-y>.
118. Brückner, A. (2022). Using weapons instead of perfume: chemical association strategies of the myrmecophilous bug *Scolopostethus pacificus* (Rhaphidochromidae). *Chemoecology* 32, 147–157. <https://doi.org/10.1007/s00049-022-00374-8>.
119. Tomalski, M.D., Blum, M.S., Jones, T.H., Fales, H.M., Howard, D.F., and Passera, L. (1987). Chemistry and functions of exocrine secretions of the ants *Tapinoma melanocephalum* and *T. erraticum*. *J. Chem. Ecol.* 13, 253–263. <https://doi.org/10.1007/BF01025886>.
120. Simon, T., and Hefetz, A. (1991). Trail-following responses of *Tapinoma simrothi* (Formicidae: Dolichoderinae) to pygidial gland extracts. *Insectes Soc.* 38, 17–25. <https://doi.org/10.1007/BF01242709>.
121. Choe, D.-H., Villafuerte, D.B., and Tsutsui, N.D. (2012). Trail pheromone of the Argentine ant, *Linepithema humile* (Mayr) (Hymenoptera: Formicidae). *PLoS One* 7, e45016. <https://doi.org/10.1371/journal.pone.0045016>.
122. Morgan, E.D. (2008). Chemical sorcery for sociality: exocrine secretions of ants (Hymenoptera: Formicidae). *Myrmecol. News* 11, 79–90.
123. Kitchen, S.A., Naragon, T.H., Brückner, A., Ladinsky, M.S., Quinodoz, S.A., Badroos, J.M., Viliunas, J.W., Kishi, Y., Wagner, J.M., Miller, D.R., et al. (2024). The genomic and cellular basis of biosynthetic innovation in rove beetles. *Cell* 187, 3563–3584.e26. <https://doi.org/10.1016/j.cell.2024.05.012>.
124. Brückner, A., Badroos, J.M., Learsch, R.W., Yousefalahiyeh, M., Kitchen, S.A., and Parker, J. (2021). Evolutionary assembly of cooperating cell types in an animal chemical defense system. *Cell* 184, 6138–6156.e28. <https://doi.org/10.1016/j.cell.2021.11.014>.
125. Wang, T.B., Patel, A., Vu, F., and Nonacs, P. (2010). Natural history observations on the velvety tree ant (*Liometopum occidentale*): unicoloniality and mating flights. *Sociobiology* 55, 787–794. <https://doi.org/10.1111/j.1558-5646.2009.00628.x>.
126. Akre, R.D., and Rettenmeyer, C.W. (1968). Trail-following by guests of army ants (Hymenoptera: Formicidae: Ecitonini). *J. Kans. Entomol. Soc.* 41, 165–174.
127. Quinet, Y., and Pasteels, J.M. (1995). Trail following and stowaway behaviour of the myrmecophilous staphylinid beetle, *Homoeusa acuminata*, during foraging trips of its host *Lasius fuliginosus* (Hymenoptera: Formicidae). *Insectes Soc.* 42, 31–44. <https://doi.org/10.1007/BF01245697>.
128. Dejean, A., and Beugnon, G. (1996). Host-ant trail following by myrmecophilous larvae of Liphyrinae (Lepidoptera, Lycaenidae). *Oecologia* 106, 57–62. <https://doi.org/10.1007/BF00334407>.
129. Moore, W., Scarpato, G., and Di Giulio, A.D. (2022). Foe to frenemy: predacious ant nest beetles use multiple strategies to fully integrate into ant nests. *Curr. Opin. Insect Sci.* 52, 100921. <https://doi.org/10.1016/j.cois.2022.100921>.
130. Borowiec, M.L., Rabeling, C., Brady, S.G., Fisher, B.L., Schultz, T.R., and Ward, P.S. (2019). Compositional heterogeneity and outgroup choice influence the internal phylogeny of the ants. *Mol. Phylogenet. Evol.* 134, 111–121. <https://doi.org/10.1016/j.ympev.2019.01.024>.
131. Tang, W., and Bennett, D.A. (2010). Agent-based modeling of animal movement: a review. *Geogr. Compass* 4, 682–700. <https://doi.org/10.1111/j.1749-8198.2010.00337.x>.
132. Hoey-Chamberlain, R., and Rust, M.K. (2014). The survivorship and water loss of *Liometopum luctuosum* (Hymenoptera: Formicidae) and *Liometopum occidentale* (Hymenoptera: Formicidae) exposed to different temperatures and relative humidity. *J. Insect Sci.* 14, 249. <https://doi.org/10.1093/jisesa/ieu111>.
133. Hölldobler, B. (1969). Host finding by odor in the myrmecophilic beetle *Atemeles pubicollis* Bris. (Staphylinidae). *Science* 166, 757–758. <https://doi.org/10.1126/science.166.3906.757>.
134. Auer, T.O., Shahandeh, M.P., and Benton, R. (2021). *Drosophila sechellia*: a genetic model for behavioral evolution and neuroecology. *Annu. Rev. Genet.* 55, 527–554. <https://doi.org/10.1146/annurev-genet-071719-020719>.
135. Dicke, M. (2000). Chemical ecology of host-plant selection by herbivorous arthropods: a multitrophic perspective. *Biochem. Syst. Ecol.* 28, 601–617. [https://doi.org/10.1016/S0305-1978\(99\)00106-4](https://doi.org/10.1016/S0305-1978(99)00106-4).

136. Janzen, D.H. (1985). On ecological fitting. *Oikos* 45, 308. <https://doi.org/10.2307/3565565>.
137. Agosta, S.J., and Klemens, J.A. (2008). Ecological fitting by phenotypically flexible genotypes: implications for species associations, community assembly and evolution. *Ecol. Lett.* 11, 1123–1134. <https://doi.org/10.1111/j.1461-0248.2008.01237.x>.
138. Klimov, P.B., O'Connor, B.M., and Knowles, L.L. (2007). Museum specimens and phylogenies elucidate ecology's role in coevolutionary associations between mites and their bee hosts. *Evolution* 61, 1368–1379. <https://doi.org/10.1111/j.1558-5646.2007.00119.x>.
139. Tishechkin, A.K. (2007). Phylogenetic revision of the genus *Mesynodites* (Coleoptera: Histeridae: Hetaerinae) with descriptions of new tribes, genera and species. *Sociobiology* 49, 5–167.
140. Bruyndonckx, N., Dubey, S., Ruedi, M., and Christe, P. (2009). Molecular phylogenetic relationships between European bats and their ectoparasitic mites (Acari, Spinturnicidae). *Mol. Phylogenet. Evol.* 51, 227–237. <https://doi.org/10.1016/j.ympev.2009.02.005>.
141. Klimov, P.B., Mironov, S.V., and O'Connor, B.M. (2017). Detecting ancient codispersals and host shifts by double dating of host and parasite phylogenies: Application in proctophyllid feather mites associated with passerine birds. *Evolution* 71, 2381–2397. <https://doi.org/10.1111/evo.13309>.
142. Peters, R.S., Niehuis, O., Gunkel, S., Bläser, M., Mayer, C., Podsiadlowski, L., Kozlov, A., Donath, A., van Noort, S., Liu, S., et al. (2018). Transcriptome sequence-based phylogeny of chalcidoid wasps (Hymenoptera: Chalcidoidea) reveals a history of rapid radiations, convergence, and evolutionary success. *Mol. Phylogenet. Evol.* 120, 286–296. <https://doi.org/10.1016/j.ympev.2017.12.005>.
143. Stireman, J.O., Cerretti, P., O'Hara, J.E., Blaschke, J.D., and Moulton, J.K. (2019). Molecular phylogeny and evolution of world Tachinidae (Diptera). *Mol. Phylogenet. Evol.* 139, 106358. <https://doi.org/10.1016/j.ympev.2018.12.002>.
144. Lähteenaro, M., Benda, D., Straka, J., Nylander, J.A.A., and Bergsten, J. (2024). Phylogenomic analysis of *Stylops* reveals the evolutionary history of a Holarctic Strepsiptera radiation parasitizing wild bees. *Mol. Phylogenet. Evol.* 195, 108068. <https://doi.org/10.1016/j.ympev.2024.108068>.
145. Dick, C.W., Esbérard, C.E.L., Gracioli, G., Bergallo, H.G., and Gettinger, D. (2009). Assessing host specificity of obligate ectoparasites in the absence of dispersal barriers. *Parasitol. Res.* 105, 1345–1349. <https://doi.org/10.1007/s00436-009-1563-1>.
146. Clayton, D.H., Bush, S.E., Goates, B.M., and Johnson, K.P. (2003). Host defense reinforces host-parasite cospeciation. *Proc. Natl. Acad. Sci. USA* 100, 15694–15699. <https://doi.org/10.1073/pnas.2533751100>.
147. Bush, S.E., and Clayton, D.H. (2006). The role of body size in host specificity: reciprocal transfer experiments with feather lice. *Evolution* 60, 2158–2167. <https://doi.org/10.1111/j.0014-3820.2006.tb01853.x>.
148. Desneux, N., Barta, R.J., Hoelmer, K.A., Hopper, K.R., and Heimpel, G.E. (2009). Multifaceted determinants of host specificity in an aphid parasitoid. *Oecologia* 160, 387–398. <https://doi.org/10.1007/s00442-009-1289-x>.
149. Casacci, L.P., Schönrogge, K., Thomas, J.A., Balletto, E., Bonelli, S., and Barbero, F. (2019). Host specificity pattern and chemical deception in a social parasite of ants. *Sci. Rep.* 9, 1619. <https://doi.org/10.1038/s41598-018-38172-4>.
150. Bois, J. (2020). *bebi103*: 0.1.0. <https://doi.org/10.22002/d1.1615>.
151. Bois, J.S. (2022). *iqplot*: 0.3.2. <https://doi.org/10.22002/d1.20286>.
152. Harris, C.R., Millman, K.J., Walt, S.J., van der Gommers, R., Virtanen, P., Cournapeau, D., Wieser, E., Taylor, J., Berg, S., Smith, N.J., et al. (2020). Array programming with NumPy. *Nature* 585, 357–362. <https://doi.org/10.1038/s41586-020-2649-2>.
153. McKinney, W. (2010). Data structures for statistical computing in Python. Proceedings of the 9th Python Sci. Conf. 56–61. <https://doi.org/10.25080/Majors-92bf1922-00a>.
154. Goloborodko, A.A., Levitsky, L.I., Ivanov, M.V., and Gorshkov, M.V. (2013). Pyteomics—a Python framework for exploratory data analysis and rapid software prototyping in proteomics. *J. Am. Soc. Mass Spectrom.* 24, 301–304. <https://doi.org/10.1007/s13361-012-0516-6>.
155. Levitsky, L.I., Klein, J.A., Ivanov, M.V., and Gorshkov, M.V. (2019). Pyteomics 4.0: five years of development of a Python proteomics framework. *J. Proteome Res.* 18, 709–714. <https://doi.org/10.1021/acs.jproteome.8b00717>.
156. van der Walt, S., Schönberger, J.L., Nunez-Iglesias, J., Boulogne, F., Warner, J.D., Yager, N., Gouillart, E., and Yu, T.; scikit-image contributors (2014). scikit-image: image processing in Python. *PeerJ* 2, e453. <https://doi.org/10.7717/peerj.453>.
157. Pedregosa, F., Varoquaux, G., Gramfort, A., Michel, V., Thirion, B., Grisel, O., Blondel, M., Prettenhofer, P., Weiss, R., Dubourg, V., et al. (2011). Scikit-learn: Machine Learning in Python. *J. Mach. Learn. Res.* 12, 2825–2830.
158. Hunter, J.D. (2007). Matplotlib: a 2D graphics environment. *Comput. Sci. Eng.* 9, 90–95. <https://doi.org/10.1109/MCSE.2007.55>.
159. Virtanen, P., Gommers, R., Oliphant, T.E., Haberland, M., Reddy, T., Cournapeau, D., Burovski, E., Peterson, P., Weckesser, W., Bright, J., et al. (2020). SciPy 1.0: fundamental algorithms for scientific computing in Python. *Nat. Methods* 17, 261–272. <https://doi.org/10.1038/s41592-019-0686-2>.
160. van den Boogaart, K.G., Tolosana-Delgado, R., Bren, M. (2020) compositions: Compositional Data Analysis. R package version 2.0-0. <https://doi.org/10.32614/CRAN.package.compositions>
161. Palarea-Albaladejo, J., and Martín-Fernández, J.A. (2015). zCompositions — R package for multivariate imputation of left-censored data under a compositional approach. *Chemom. Intell. Lab. Syst.* 143, 85–96. <https://doi.org/10.1016/j.chemolab.2015.02.019>.
162. Mersmann, O., Trautmann, H., Steuer, D., and Bornkamp, B. (2018). truncnorm: Truncated Normal Distribution. R package version 1.0-8. <https://doi.org/10.32614/CRAN.package.truncnorm>.
163. Lee, L. (2020). NADA: Nondetects and Data Analysis for Environmental Data. R package version 1.6-1.1. <https://doi.org/10.32614/CRAN.package.NADA>.
164. Therneau, T., Lumley, T., Atkinson, E., and Crowson, C. (2019). survival: Survival Analysis. R package version 2.44-1.1. <https://doi.org/10.32614/CRAN.package.survival>.
165. Therneau, T.M., and Grambsch, P.M. (2000). *Modeling Survival Data: Extending the Cox Model* (Springer).
166. Ripley, B., Venables, B., Bates, D.M., Hornik, K., Gebhardt, A., and Firth, D. (2020). MASS: Support Functions and Datasets for Venables and Ripley's MASS. R package version 7.3-51.6. <https://doi.org/10.32614/CRAN.package.MASS>.
167. Venables, W.N., and Ripley, B.D. (2002). *Modern Applied Statistics with S, Fourth edition* (Springer).
168. Oksanen, J., Blanchet, F.G., Kindt, R., Legendre, P., Minchin, P., O'Hara, R., Simpson, G., Solymos, P., Henry, M., Stevens, M., et al. (2015). Vegan community ecology package: ordination methods, diversity analysis and other functions for community and vegetation ecologists. R Package ver., pp 2–3.
169. Sarkar, D. (2008). *Lattice: Multivariate Data Visualization with R* (Springer).
170. Simpson, G.L., Bates, D.M., and Oksanen, J.; R Core Team (2019). permute: Functions for Generating Restricted Permutations of Data. R package version 0.9-5. <https://doi.org/10.32614/CRAN.package.permute>.
171. Bewley, A., Ge, Z., Ott, L., Ramos, F., and Upcroft, B. (2016). Simple online and realtime tracking. In *IEEE International Conference Image Processing (ICIP)*, pp. 3464–3468. <https://doi.org/10.1109/ICIP.2016.7533003>.
172. Jocher, G., Chaurasia, A., and Qiu, J. (2023) Ultralytics YOLOv8.

173. Nath, T., Mathis, A., Chen, A.C., Patel, A., Bethge, M., and Mathis, M.W. (2019). Using DeepLabCut for 3D markerless pose estimation across species and behaviors. *Nat. Protoc.* 14, 2152–2176. <https://doi.org/10.1038/s41596-019-0176-0>.
174. Comaniciu, D., Ramesh, V., and Meer, P. (2003). Kernel-based object tracking. *IEEE Trans. Pattern Anal. Mach. Intell.* 25, 564–577. <https://doi.org/10.1109/TPAMI.2003.1195991>.
175. Carlson, D.A., Bernier, U.R., and Sutton, B.D. (1998). Elution patterns from capillary GC for methyl-branched alkanes. *J. Chem. Ecol.* 24, 1845–1865. <https://doi.org/10.1023/A:1022311701355>.
176. Dembeck, L.M., Böröczky, K., Huang, W., Schal, C., Anholt, R.R.H., and Mackay, T.F.C. (2015). Genetic architecture of natural variation in cuticular hydrocarbon composition in *Drosophila melanogaster*. *eLife* 4, e09861. <https://doi.org/10.7554/eLife.09861>.
177. D'Eustacchio, D., Centorame, M., Fanfani, A., Senczuk, G., Jiménez-Alemán, G.H., Vasco-Vidal, A., Méndez, Y., Ehrlich, A., Wessjohann, L., and Francioso, A. (2019). Iridoids and volatile pheromones of *Tapinoma dariori* ants: chemical differences to the closely related species *Tapinoma magnum*. *Chemoecology* 29, 51–60. <https://doi.org/10.1007/s00049-018-00275-9>.

STAR★METHODS

KEY RESOURCES TABLE

REAGENT or RESOURCE	SOURCE	IDENTIFIER
Biological samples		
<i>Sceptobius lativentris</i>	Wild caught by authors in Angeles National Forest, California, USA	N/A
<i>Liometoxenus newtonarum</i>	Wild caught by authors and Y. Kishi in Angeles National Forest, California, USA	N/A
<i>Platyusa sonomae</i>	Wild caught by authors in Angeles National Forest, California, USA	N/A
<i>Rhopalid</i> sp.	Wild caught J. Wagner in Angeles National Forest, California, USA	N/A
<i>Scolopostethus</i> sp.	Wild caught J. Wagner in Angeles National Forest, California, USA	N/A
<i>Histerid</i> sp.	Wild caught by J. Parker, California, USA	N/A
<i>Liometopum occidentale</i>	Wild caught by authors in Angeles National Forest, California, USA	N/A
<i>Liometopum apiculatum</i>	Wild caught by J. Parker, Arizona, USA	N/A
<i>Liometopum luctuosum</i>	Wild caught by authors in San Bernardino National Forest, California, USA	N/A
<i>Veromessor andrei</i>	From lab colony collected by J. Truong or field collected by J. Wagner, California, USA	N/A
<i>Pogonomyrmex</i> sp.	From lab colony collected by J. Truong or field collected by J. Wagner, California, USA	N/A
<i>Formica</i> sp.	From lab colony collected by J. Truong, California, USA	N/A
<i>Dalotia coriaria</i>	Applied Bionomics (Canada)	https://www.appliedbio-nomics.com/products/dalotia/
<i>Drosophila melanogaster</i>	Dickinson Laboratory (Caltech)	N/A
Chemicals, peptides, and recombinant proteins		
Hexane ReagentPlus, ≥99% (for GCMS extractions)	Sigma-Aldrich	Cat# 139386
Hexane SupraSolv, ≥98% (for GCMS extractions)	Supelco	Cat# 1.00795
Octadecane, analytical standard	Supelco	Cat# 74691
sodium dodecyl sulfate, ACS Reagent grade, ≥99.0%	Sigma-Aldrich	Cat# 436143
2-propanol, ≥99.5%, for molecular biology	Sigma-Aldrich	Cat# I9516
230–400 mesh flash chromatography grade silica gel, Grade 60	Fisher Scientific	Cat# S825-25
Hexane, Optima grade (for fractionations)	Fisher Scientific	Cat# H303-4
Cyclohexene, Reagent-Plus grade, Inhibitor free	Sigma-Aldrich	Cat# 125431
Diethyl ether, ACS Reagent grade, anhydrous, stabilized with BHT	Fisher Scientific	Cat# E138-4
Ethyl acetate, Optima grade	Fisher Scientific	Cat #E136-4
Deposited data		
Data to generate all figures	This study	CaltechDATA: https://doi.org/10.22002/taxa0-k3571

(Continued on next page)

Continued

REAGENT or RESOURCE	SOURCE	IDENTIFIER
Software and algorithms		
python 3.7.7	Python Software Foundation	https://www.python.org/
bokeh 2.2.3	Bokeh Development Team	https://docs.bokeh.org/en/latest/
bebi103 0.0.54	Bois ¹⁵⁰	https://pypi.org/project/bebi103/
opencv-python 3.4.9.31	OpenCV	https://pypi.org/project/opencv-python/
iqplot 0.3.2	Justin ¹⁵¹	https://doi.org/10.22002/D1.20286
numpy 1.16.4	Harris et al. ¹⁵²	https://pypi.org/project/numpy/
pandas 1.0.3	McKinney ¹⁵³	https://pypi.org/project/pandas/
pyteomics 4.4.0	Goloborodko et al. ¹⁵⁴ and Levitsky et al. ¹⁵⁵	https://pypi.org/project/pyteomics/
scikit-image 0.17.2	Walt et al. ¹⁵⁶	https://pypi.org/project/scikit-image/
scikit-learn 0.22.2.post1	Pedregosa et al. ¹⁵⁷	https://pypi.org/project/scikit-learn/
tqdm 4.51.0	tqdm developers	https://pypi.org/project/tqdm/
jupyterlab 1.2.6	Project Jupyter	https://pypi.org/project/jupyterlab/
python 3.11.5	Python Software Foundation	https://www.python.org/
jupyterlab 4.0.8	Project Jupyter	https://pypi.org/project/jupyterlab/
bokeh 3.3.0	Bokeh Development Team	https://docs.bokeh.org/en/latest/
bebi103 0.1.17	Bois ¹⁵⁰	https://pypi.org/project/bebi103/
matplotlib 3.8.2	Hunter ¹⁵⁸	https://pypi.org/project/matplotlib/
numpy 1.26.2	Harris and Millman ¹⁵²	https://pypi.org/project/numpy/
pandas 2.1.3	McKinney ¹⁵³	https://pypi.org/project/pandas/
scipy 1.11.4	Virtanen et al. ¹⁵⁹	https://pypi.org/project/scipy/
R version 3.6.1	R Core Team	https://www.R-project.org/
compositions 2.0-0	van den Boogaart et al. ¹⁶⁰	https://cran.r-project.org/package=compositions
zCompositions 1.3.4	Palarea-Albaladejo and Martín-Fernández ¹⁶¹	https://github.com/Japal/zCompositions
truncnorm 1.0-8	Mersmann et al. ¹⁶²	https://cran.r-project.org/package=truncnorm
NADA 1.6-1.1	Lopaka Lee ¹⁶³	https://cran.r-project.org/package=NADA
survival 2.44-1.1	Therneau et al. ^{164,165}	https://cran.r-project.org/package=survival
MASS 7.3-51.6	Ripley et al. ^{166,167}	https://cran.r-project.org/package=MASS
vegan 2.5-6	Oksanen et al. ¹⁶⁸	https://cran.r-project.org/package=vegan
lattice 0.20-41	Sarkar et al. ¹⁶⁹	https://cran.r-project.org/package=lattice
permute 0.9-5	Simpson et al. ¹⁷⁰	https://cran.r-project.org/package=permute
Matlab R2023a, version 9.14	The MathWorks Inc.	https://www.mathworks.com
SORT	Bewley et al. ¹⁷¹	https://github.com/abewley/sort
CVAT	CVAT.ai Corporation	https://www.cvat.ai/
YOLOv8	Jocher et al. ¹⁷²	https://docs.ultralytics.com/models/yolov8/
DeepLabCut 2.2b6	Mathis et al., ¹¹⁷ DeepLabCut, ²¹ Nath et al., ¹⁷³ and Caves et al., ¹⁴	https://github.com/DeepLabCut/DeepLabCut
GCMSsolution Version 4.45	Shimadzu Corporation	https://www.ssi.shimadzu.com/products/gas-chromatograph-mass-spectrometry/gc-ms-software/gcmsolution/index.html
Data analysis scripts	This Study	CaltechDATA: https://doi.org/10.22002/taxa0-k3571
Other		
GCMS-QP2020 gas chromatography/mass-spectrometry system	Shimadzu	GCMS-QP2020
ZB-5MS fused silica capillary column for GCMS	Phenomenex	7HG-G010-11
Mono camera: BFS-U3-63S4M-C 6.3 MP	Flir	BFS-U3-63S4M-C

(Continued on next page)

Continued

REAGENT or RESOURCE	SOURCE	IDENTIFIER
Mono camera: BFS-U3-16S2M-CS: 1.6 MP	Flir	BFS-U3-16S2M-CS
Mono camera: BFS-U3-51S5M-C: 5.0 MP	Flir	BFS-U3-51S5M-C
Color camera: BFS-U3-51S5M-C: 5.0 MP	Flir	BFS-U3-51S5C-C
Color camera: BFS-U3-200S6C-C: 20 MP	Flir	BFS-U3-200S6C-C
FLIR Lepton 2.5	Flir	Model: 500-0763-01
FLIR Purethermal-2	Flir	PURETHERMAL-2
Pentax 12mm 1:1.2 TV lens	Ricoh	FL-HC1212B-VG
Pentax C61232KP 12mm F1.4 Manual Lens with Lock Screw	Pentax	C61232KP
16mm 10MP Telephoto Lens for a Raspberry Pi HQ Camera	Adafruit	Product ID: 4562
0.118" X 48" X 96" 3143 Plexiglass Infrared Transmitting Acrylic Sheet	ePlastics	ACRY31430.125PM48X96
Prusa I3 MK2 3d printer	Prusa Research	I3 MK2

EXPERIMENTAL MODEL AND STUDY PARTICIPANT DETAILS

Animals used for behavioral studies were primarily wild caught, or from ant colonies grown in the lab from wild caught queens. The exceptions are *D. coriaria* and *D. melanogaster* which were collected from bulk cultures maintained in the lab and for which males and females were randomly selected. All ants used were female adults (all workers are female) of unknown age since this is not possible to estimate for wild caught animals. For all the wild caught non-ant interactor insects (all but *D. melanogaster* and *D. coriaria*), we did not sex individuals used in the assays as there is no clear way to do so with these organisms since they are scarcely studied. For *S. lativentris*, age was also not possible to determine, and we used males for all our grooming behavioral trials (dense spatulate bristles on antennomere 3 are present in males only). Though the females looked to behave identically in lab colonies and in a limited set of behavioral trials, we wanted to control for whether animals were egg bearing, and sex was one of the only organismal variables we were able to control since we wild caught the beetles and they are currently not culturable in lab. For trail following experiments, a mix of male and female beetles were used, and we observed no apparent differences in behavior between the sexes.

METHOD DETAILS

Specimen collection and husbandry of *S. lativentris* and *L. occidentale*

Beetles and ants were collected in the Angeles National Forest, primarily near the parking lot of Chaney trail and along Millard creek in Altadena, CA (34.2163413, -118.146500), and near Gould Mesa Trail camp, along Gabrieleno trail, also near to a creek (34.2222252, -118.1785464). *Liometopum occidentale* builds nests in the bases of oak (*Quercus*, especially *Quercus agrifolia* at the listed collecting sites) and bay trees (*Umbellularia californica*). In warmer/drier conditions (especially during the summer) leaf litter near to ant nests and along foraging trails was sifted, and the trays examined for beetles. During colder weather and early in the spring, beetles walk on the trees housing the ant nest, often near the nest opening. Blowing exhaled air into an undisturbed nest often increases activity, enabling collection of *S. lativentris* exiting the nest. Beetles were captured via aspirator and placed with host ants in falcon tubes with slightly dampened KimWipes. *S. lativentris* are abundant, and could be collected during most of the year, but are more difficult to find during November–January. Collecting expeditions yielded as few as zero beetles on the coldest days, compared with up to ~200 beetles per colony per day during later spring and summer. To keep *S. lativentris* in the laboratory, beetles were housed with an excess of well-fed *L. occidentale* workers collected from the same colony that yielded the beetles. In the laboratory, beetles were placed with host ants into ~25 cm x 25 cm Rubbermaid boxes with a Fluon barrier (2/3 water, 1/3 Insect-a-Slip) painted on the sides to avoid escape. Animals were provided a feeder of hummingbird nectar (4 parts water, 1 part nectar) and a test tube setup with water and cotton balls to provide moisture. Specimens housed this way survived up to several months in the laboratory. *Sceptrubius lativentris* were sexed for experiments based on a dimorphism in antennal setation: males have a high density of spatulate setae on antennomere 3, whereas females have few such setae. Ice was used as an anesthetic for sexing beetles under the microscope and sorting them for experiments (CO₂ anesthesia was found to cause mortality).

Grooming behavioral arenas

Grooming Arena 1

A multiplexed array of circular arenas was constructed to record grooming behavior (Figure S2A). To avoid vision influencing behavior, behavioral arenas were constructed out of 3.18 mm infrared-transmitting acrylic (Plexiglass IR acrylic 3143) which transmits far red and infrared while blocking visible light. Hence, experimental trials were conducted in darkness. Arenas consisted of a

base layer of finely wet-sanded acrylic (to provide a texture on which beetles could walk), on top of which was placed a second layer with multiple, 2 cm diameter, circular wells. Finally, a top acrylic roof layer was added to contain the animals inside the arena. Slight modifications of these 2 cm arenas were used throughout the data collection period, with either fixed-well shape or a sliding door design to allow a particular start time for insect interactions. Behavioral interactions were run in a dark incubator, situated within a dedicated behavior room with the lights switched off, behind a blackout curtain to further ensure that the insects were behaving in complete darkness. Arenas were backlit with a custom-built IR850nm LED PCB and diffused with a semi-opaque white acrylic sheet. Recordings of interactions were made using a FLIR machine vision camera (BFS-U3-51S5M-C: 5.0 MP) at 3 frames per second with a Pentax 12mm 1:1.2 TV lens (by Ricoh, FL-HC1212B-VG), for 6 hours.

Grooming Arena 2

Similar arenas as above were also built (Figure S2B), but designed with side rather than top IR illumination, a higher camera frame rate, and higher resolution per experimental well to better maintain visibility of the beetle when grooming during trials, and provide more information-rich behavioral data. For this second setup, an 8-well arena with similar design as mentioned above was used, with a base layer of sanded IR acrylic, a wall layer with eight 2 cm circular arena cutouts, a ceiling of static dissipating acrylic with a rim of IR acrylic, and a second roof of IR-transmitting acrylic. All acrylic used here was 3.18 mm thick. An aluminum frame to hold the arena was constructed with 1 inch (2.54 cm) T-slotted framing from McMaster-Carr, along with open gusset structural brackets, and custom laser-cut brackets made of 6.35 mm acrylic. IR flood lights (Univiv U6R) were side-mounted, and a FLIR machine vision camera (BFS-U3-51S5M-C: 5.0 MP) with a Pentax 12mm 1:1.2 TV lens (by Ricoh, FL-HC1212B-VG), was used to record at 60 frames per second. An Arduino-based external trigger was also used to maintain the frame rate of the camera. The arena was placed in a dark, temperature-controlled incubator set to 18°C. A thermal camera (FLIR Lepton 2.5 with FLIR Purethermal-2), was used to determine that the arena itself, heated by the IR lights, maintained a consistent temperature of 21°C during the trials.

Loading arenas and preparing behavioral experiments

To control for sex differences, only male *S. lativentris* were used for all grooming experiments (although female beetles exhibit overtly identical grooming behavior). Beetles were isolated in a container with two moistened KimWipes for 30 minutes–1 hour before loading into behavioral arenas. Beetles and interactor ants/insects were anesthetized on ice for 10 minutes before loading into a pre-chilled arena in a 4°C refrigerator to prevent them escaping. Loaded arenas were then placed into the incubator setup as described above and recording started. In the case of sliding door arenas, arena pieces were slid together to start interactions after *S. lativentris* started moving around its arena well, ~10 minutes after beginning the loading process.

Machine learning analysis of grooming behavior

DeepLabCut for grooming arena analysis

DeepLabCut^{117,173} was used to track beetle and ant/other insect behavior. A network model with five labeled points on the *S. lativentris* and five labeled points on each interactor was used (Figure S2C). We found that a single model to detect these key points could be trained to identify the beetle and the other insect, regardless of the species by including additional training frames to the dataset for each interactor type. A ResNet50 network architecture was trained and subsequently used for annotation. The final network was trained on ~2300 frames from more than 200 videos. This network achieved an error of 2.53 pixels for the training data, and 4.45 for the test data, which represents an error of less than 1/5th of a mm within the arena (less for most videos). Videos for grooming experiments were analyzed at a temporal resolution of 3 frames per second. If no detection for a given animal was present in a frame, linear interpolation from the last known position to the next known detection position was used to fill the gap. The distance between the beetle and the other interactor insect was calculated during the trial, and an interaction was considered a grooming bout if the beetle was within 3 mm of the ant for at least 30 seconds. Processing and plotting of key point data, as well as work with other metadata and raw data in the paper, was done in python and heavily employed numpy¹⁵² for array and mathematical operations and pandas dataframes to store and access data. Plotting of categorical data (e.g. Figure 2G) was also done in python with bokeh and the iqplot package by Justin Bois.¹⁵¹ All code for such analysis and plotting is available and linked in the Resource Availability section above.

YOLOv8 preference assay analysis

To test whether *S. lativentris* showed a preference for grooming its host ant over other ants, a single *L. occidentale* host ant worker and either a single sister ant (*L. luctuosum*) or a phylogenetically divergent ant (*V. andrei*) were placed with a single beetle in an arena well. To quantify the relative preference for one ant species over the other, the amount of time the beetle spent grooming each ant during a two- or six-hour trial was determined. For analysis, behavioral videos were subsampled to one frame per 16.7 seconds. YOLOv8¹⁷² was used for detection and bounding box generation of the location of each ant and each beetle during the behavioral trial (Figures S4A and S4B). Frames were extracted uniformly from each behavioral trial video (10 per video for the *L. luctuosum* analysis for a total of 480 frames from 48 trials, or 30/31 per video for the *V. andrei* analysis for a total of 481 frames labeled). An 85% training data -15% validation data split was used. Labeled data with a bounding box per animal were manually generated in CVAT (<https://www.cvat.ai/>). The network was trained with YOLOv8's default settings (epochs: 100, patience: 50, batch: 16, imgsiz: 640, lr0: 0.01, lrf: 0.01, momentum: 0.937, weight_decay: 0.0005, warmup_epochs: 3.0, warmup_momentum: 0.8, warmup_bias_lr: 0.1, etc.) (see Figures S4A and S4B for training results). Detection was then performed on all frames of the subsampled behavioral videos. For each frame, the highest confidence detection for each animal type per frame was taken. If no detection for a given animal was present in a frame, linear interpolation from the last known position to the next known detection position was used to fill in gaps. The distance between the beetle and the other interactors during the trial was calculated, and considered a grooming interaction if the

beetle was within 3 mm of the ant for at least 90 seconds. Due to the lower temporal resolution of the annotated frames used to speed the computations for this analysis (1 frame per 16.7 seconds), we used the mentioned 90 second interaction threshold to call grooming instead of the 30 second threshold used for the DeepLabCut analysis. The reason for this difference is that the 90 second threshold requires evidence from at least six subsequent frames to call a grooming bout instead of just two frames which a 30 second threshold would require; hence, we took the slightly more conservative 90 second threshold. To estimate the amount of time grooming each individual ant type, ambiguous grooming bouts where the beetle was within 3 mm of both ants were eliminated, and the cumulative time spent grooming just one or the other ant species unambiguously was calculated. To quantify preference, total groom times for each ant species were subtracted to obtain a differential groom time estimate.

Trail following analysis

Naturally laid trail arena

To assay trail-following ability and specificity of *S. lativentris*, a large (40 × 50 cm) open field behavioral arena was constructed, enclosed within IR-transmitting acrylic (Figure S3A). To provide a naturalistic ant-trail stimulus, ants from a laboratory colony of *L. occidentale* were allowed to lay down a trail in the arena, with a large sheet of filter paper covering the bottom of the arena, both to capture ant pheromones and to act as a diffuser for the IR 850nm strip backlights. After starving the ants for 2 days, the colony was connected to the arena environment, with a foraging object (sugar water) available at a distal region of the arena (Figure S3A). Within the free field arena, obstacles were placed to force the ants to lay a trail with a specific geometry. After allowing the ants to forage for 12 hr, the ant colony was disconnected, the arena was filled with CO₂ to anesthetize remaining ants, and all ants and obstacles were removed from the arena (Figures S3B and S3C). The trail-bearing filter paper was placed back into the arena, and single *L. occidentale* workers (Figure S3D), *S. lativentris* beetles (Figure S3E), or free-living *Dalotia coriara* beetles (Figure S3F) were then placed into the arena and recorded for approximately 2 hours. Insect movement traces were recorded with a FLIR machine vision camera (BFS-U3-51S5M-C: 5.0 MP) with a Pentax 12mm 1:1.2 TV lens (Ricoh, FL-HC1212B-VG). To quantify trail following of individual insects, net frame-to-frame movement in the arena was correlated with ant movement flow at that position in the arena. Frame-to-frame beetle or ant movement was calculated based on thresholding the difference between subsequent frames to find locations of optical flow and then summed all such thresholded frames across the entire video to generate a histogram of location and amount of movement which occurred during the two hour trial. We then summed total movement within ~0.7x0.7cm area squares in the arena and normalized the resulting histogram to give the probability that a given insect was moving in a given square of the arena during the trial (the binned histograms are depicted in Figure 3A). This summing within the square areas to generate the histogram was done with the scikit-image package¹⁵⁶ in python. This gave a discrete probability distribution for movement in sections of the arena for every individual insect as well as bulk ants after laying a foraging trail. We compared how close individual insect movement distributions were to bulk ant trails using a metric related to the Bhattacharyya coefficient,¹⁷⁴ the Hellinger distance, namely

$$d(A, O) = \sqrt{1 - BC(A, O)},$$

where

$$BC(A, O) = \sum_{i=1}^n \sqrt{A_i O_i}.$$

d is the distance between probability distributions, A is the bulk ant movement probability distribution, O is the other, single insect movement probability distribution, and BC is the Bhattacharyya coefficient. Visualization of the movement was done in python with bokeh (e.g. Figure 3A) or with the bebi103 package by Justin Bois¹⁵⁰ (e.g. Figure S3B). In addition to quantifying net movement of the beetles via frame-to-frame difference, blob tracking on beetle position throughout a behavioral trial was also performed. For this, median filtering was carried out on a set of frames from the beetle-walking-in-trail-arena video to construct a background frame. With OpenCV, blob detection was performed on background-subtracted frames from the video. The median position of the blob was used to make a trajectory for beetle position in the arena.

Multi-well trail arena

To probe the chemicals relevant for trail following, a multiplexed assay to test beetle behavior in response to artificially applied trails was also developed (Figure S3H). An arena with nine square wells of 8.9 cm × 8.9 cm was constructed. The arena was constructed from stacked layers of acrylic. The base was 6.35 mm clear acrylic, with an a 3.18 mm thick layer of Plexiglass IR acrylic 3143 placed on top to block visible light. On to this was placed an IR-transmitting acrylic layer with a 30.5-cm × 30.5-cm opening that fitted a 30.5-cm × 30.5-cm square of 3.18mm thick glass with a ground surface to provide grip for beetles to walk. An opaque white acrylic layer with nine wells of 8.9 × 8.9 cm was placed onto this, with Fluon applied to the walls of each well to prevent insects from climbing onto the roof. The roof was placed over this, comprising a 3.18 mm layer of static-dissipating acrylic with a further 3.18 mm layer of IR acrylic to block visible light, and an additional 6.35 mm layer of clear acrylic to weigh down the ceiling and keep it flat. The layers were all held together by screws affixed to a metal frame and backlit with IR 850nm strip LED lights. The arena was monitored with a FLIR machine vision camera (BFS-U3-16S2M-CS: 1.6 MP) with a Pentax 12mm 1:1.2 TV lens (by Ricoh, FL-HC1212B-VG). Extracted ant compounds were painted onto a ground glass floor in a circular pattern within each well. Behavioral trials within this arena were two hours long.

To analyze the resulting videos, OpenCV was used. First, videos were cropped to extract individual wells from the array. Individual wells were warped to square them from any small camera distortions and set to a constant resolution of 320×320 pixels per well. A background frame was then constructed via median filtering of a set of images from the given well. Background subtraction was then performed for each well, and the OpenCV blob detection method was used to threshold each frame and locate the beetle (Figure S3I). The position of the beetle in the well was saved. To calculate the degree of trail following observed in the trial, the positional information given by blob tracking was used, and circular arcs within the animal trajectory extracted. To do this, regions of interest were defined as sections along the circular chemical trail of approximately 0.5 cm, moving along the circle and diverging from the trail by ~ 0.5 cm either side of the path of the circle. Twelve such regions were defined per circle, at intervals of 30° along the circle (Figure S3I). Instances where an animal traversed through these twelve regions sequentially, from one to the next, for an entire revolution of the circle were measured. Each such traversal was counted as a single circular trail following event. The distance traveled while the animals were traversing these circles was then calculated.

Preference assay in trail arena

To test whether *S. lativentris* prefers trails of its host ant over its sister ant species, a variant of the multi-well trail arena was used (Figure S6A). An approximate concentration match of crude extract from the host ant *L. occidentale* or the sister species *L. luctuosum* were prepared. To do this, hundreds of ants of the two species were extracted in hexane, and an aliquot of 2 microliters injected into a GCMS; the region of a GCMS trace (GCMS methods described elsewhere) representing the iridoid fraction of the trace was integrated to approximate the concentration of these compounds. These values were used to mix approximately equal concentration solutions of each extract. A dilution to $1/5^{\text{th}}$ the concentration was also made to generate a comparably low and high concentration extract for the host and sister ants. Abutting lobes of semi-circular trail were then painted with low or high concentration of extract from the two different ant species. A single beetle was then placed in each arena with the high-low concentration trails and its movement was recorded for a two-hour trial. For this assay the same setup as described above for the multi-well trail arena was used (Figure S3H), but with a BFS-U3-63S4M-C 6.3 MP camera with a Pentax C61232KP 12mm F1.4 Manual Lens with Lock Screw. To quantify the results, movement of the animals during the trial, the cumulative pixel difference between subsequent frames was calculated for the whole experiment. Regions of interest (ROI) were then manually defined as the arms of the trail lobes belonging to either species. The total movement in each of these ROIs was summed and subtracted to see the difference in total movement during the trial on one trail lobe or the other, which was used as a trail preference index. Example depictions of the total movement histogram and the movement histogram for a given trail lobe ROI are shown (Figure S6B).

Identification of chemical compounds and analysis of CHC profiles

For identification and profiling of chemical compounds from insect species used in this study, we used gas chromatography mass spectrometry methods described previously in Brückner et al.¹²⁴ and Kitchen et al.¹²³ Specimens were freeze killed at -80°C and stored at -20°C until extraction. Compounds were extracted by submerging individual insects in 70 microliters of hexane (SupraSolv n-Hexane, Merk or ReagentPlus n-Hexane, Sigma-Aldrich) containing 10 ng/microliter octadecane (Sigma Aldrich) as an internal standard. After 20 minutes, the hexane was transferred to a 250 μL glass small volume insert and samples were either analyzed immediately or stored at -80°C until analysis. Analysis was performed on a GCMS-QP2020 gas chromatography/mass-spectrometry system (Shimadzu, Kyōto, Japan) equipped with a Phenomenex (Torrance, CA, USA) ZB-5MS fused silica capillary column (30 m \times 0.25 mmID, $\text{df}=0.25\ \mu\text{m}$). Samples were injected (2 μL) into a split/splitless-injection port operated in splitless-mode at 310°C . Helium was used as a carrier gas with a constant flow rate of 2.15 mL/min. The column was held at 40°C for 1 min, ramped at $20^\circ\text{C}/\text{min}$ up to 250°C , ramped at $5^\circ\text{C}/\text{min}$ up to 320°C , and then held at 320°C for 7.5 minutes. The transfer line and MS ion source temperatures were kept at 320°C and 230°C respectively. Electron impact ionization was carried out at an ion source voltage of 70 eV, collecting 2 scans/sec from m/z 40 to 650.

CHCs were identified based on their fragmentation patterns and retention indices compared to a standard series of n-alkanes,¹⁷⁵ by comparison to library spectra (NIST 14 library), and comparison of retention indices and fragmentation patterns to known compounds in *Drosophila melanogaster*¹⁷⁶ and *Liometopum occidentale*.¹¹⁸ These identification tasks were done in the Shimadzu GCMSsolution software, version 4.45. Unless specified, the double-bond positions for most alkenes, dienes, and trienes were not determined. Semi-quantification of CHC amounts was carried out by calculating the ratio of each hydrocarbon peak to the C18 internal standard. Absolute amounts and percent composition were calculated for CHCs in all GC traces. The centered log-ratio transformation (abbreviated as CLR/clr in Figures 4E and 6G respectively) was applied to percent composition data following zero replacement (as needed) with the R package zCompositions¹⁶¹ before performing PCA for Figure 4E. For Figure 6G, a similar procedure was used, but since no zero replacement was required PCA analysis was performed with the scikit-learn package¹⁵⁷ in python. A subset of the total CHCs were used in the PCA analysis. Pairwise Bray-Curtis dissimilarity was calculated for untransformed percent composition data for all samples prior to performing non-metric multidimension scaling (NMDS) for Figures 2H and 4I. NMDS was performed using the metaMDS function from the R package vegan.¹⁶⁸

To plot GCMS spectrum in python (Figure 4D), mass spectrometry data was first exported into the open source mzXML format in the Shimadzu GCMSsolution software. These files were then loaded into python using the pyteomics package.^{154,155} Ion counts at each retention time were then summed to generate a chromatogram, which was then normalized for plotting. The resulting chromatogram was plotted with bokeh.

Iridoids were identified by comparison to library spectra (NIST 14 library) and by comparison of fragmentation patterns and retention indices to previously described iridoids in ants.¹⁷⁷ Both iridodial and nepetalactol possess multiple stereocenters and while we

were able to determine that multiple stereoisomers for both compounds were present, we could not identify the exact configuration of the compounds.

Fractionation of ant chemical compounds

A bulk hexane extraction of tens of thousands of *L. occidentale* workers was made, with a concentration estimated of ~50-100 ants per ml. This stock extract was stored at -20°C. 50 ml of extract was concentrated to dryness by rotary evaporation, and the residue re-dissolved in 5 ml hexane. A vacuum flash chromatography column was prepared from a 10 ml sintered glass funnel filled with 230-400 mesh flash chromatography grade silica gel. The silica gel bed was packed with hexane by pulling the solvent through with vacuum. The hexane solution of concentrated ant extract was loaded onto the column, rinsing with hexane. The column was eluted sequentially with:

- 3 x 12 ml hexane
- 3 x 12 ml 5% cyclohexene in hexane
- 2 x 12 ml ether
- 2 x 12 ml EtOAc

This method accomplished the fractionation, leaving saturated hydrocarbons in fraction 1 and 2, unsaturated hydrocarbons in fractions 5 and 6, and polar compounds in fractions 7 and 8. Fractions 1 and 2 were combined, as well as 5 and 6, and 7-10, and volumes adjusted to 10 ml, or ~250 ant equivalents/ml. The polar and non-polar fractions were used for experiments.

Agent-based modeling

An *in silico* agent-based simulation was designed to reproduce *Sceptobius* interactions with host and non-host ants across a virtual landscape. The model incorporates two core limitations on beetle survival: i) intrinsic mortality due to CHC loss and other isolation-related sources of death; and ii) extrinsic mortality caused by encounters with ants that diverge from the beetle's own, current CHC profile, with greater divergence inversely related to beetle survival probability. We built models in Matlab, where $N \times N$ grids of variable size are instantiated representing a 2D forest floor through which beetles and ants navigate. Host colony (Colony A) and non-host (Colony B) are located at opposite corners of the forest grid. In each simulation, all beetles start within colony A, and all ants start within their respective colonies. The beetles also start with a full supply of CHCs: for the purpose of the model, we encoded two CHCs, one for recognition, and one for resistance to desiccation. Both CHCs are lost at a rate ΔCHC_{loss} when beetles are isolated from ants, the value of which was varied across *in silico* runs. At each step of the simulation, each ant moves to one of the four squares contiguous with its current squares. The probability of movement was biased such that ants further away from their source colony were relatively more likely to move backwards to a square closer to the nest. When an ant from Colony A encounters an ant from Colony B, the winning species is determined by a coin flip. If ants from one Colony outnumber ants from the other within a square, the outnumbered ants die. At each time step, the beetles also move within the arena and lose their CHCs at the rate ΔCHC_{loss} . When beetles encounter an ant with the same CHCs it possesses ($\Delta CHC_{ID} = 0$), it grooms, re-gaining full quantities of both recognition and desiccation-resistance CHCs. When beetles encounter a novel, non-host ant with divergent CHCs to its own ($\Delta CHC_{ID} \neq 0$), its probability of being killed is function of both the degree of CHC divergence (ΔCHC_{ID}) and the total amount of CHCs on its body (ΣCHC). If the beetle survives the encounter, it replenishes its CHCs and changes its recognition CHC to the identity of the novel, chemically divergent ant. The probability that the beetle survives the encounter is given by:

$$p(killed) = \frac{1}{\left(1 + 50 * e^{-0.5 * \left(1 + \frac{\# \text{ ants}}{10}\right) * \text{aggressiveness}_{\text{ant}} * \text{CHC}_{\text{beetle}}}\right)^2}$$

When ants or beetles die, they are reborn at their starting colony to keep the number of animals in the simulation constant. We ran each simulation for 1000 steps, and screened through parameter space, repeating each set of parameter values 100 times to converge on average outcomes for each set of conditions. The simulation was run across a spectrum of CHC loss rates (ΔCHC_{loss}), degrees of non-host ant aggressiveness (ΔCHC_{ID}), and different inter-colony distances by varying the forest floor arena area. In each case, we recorded how these parameters influence i) the frequency and cause of beetle death (intrinsic versus extrinsic mortality); ii) the probability beetles successfully obtain CHCs from non-host ants, and iii) the probability beetles were able to host switch to the non-host colony. Results from the Matlab model were loaded into python using scipy,¹⁵⁹ and matrices plotted with bokeh with color palettes generated using matplotlib.¹⁵⁸

Host-switching behavioral platforms

To experimentally test the *in silico* model of host switching, arenas were constructed that matched the design of the model.

Cross arena

To recreate beetle interactions with opposing colonies of host and non-host ants, we constructed an arena area comprised two nest chambers flanking a central dispersal arena (Figure S7B). Beetles and varying numbers of ants of two different species were placed into the nest chambers and were permitted to disperse into a central area comprising a 20×20 grid of cross-shaped separators that

formed an array of connected wells in which the ants and beetles could interact. The cross-arena plate design was printed with a Prusa I3 MK2 3d printer in clear PLA. The base of the piece was 3.18 mm thick, and the wall component also 3.18 mm thick. Acrylic was used to sandwich the 3D printed component and provide a ceiling to contain the animals. Screw holes were cut into a base plate of 3.18 mm clear acrylic, matching holes in two 3.18 mm pieces with cutouts of the same dimensions as the arena, and a ceiling of clear acrylic. This created a 4-layer sandwich encasing the arena. Two such arenas were mounted next to each other in a metal frame. We maintained color information in these trials to help differentiate ants of different species and the beetles. We placed white LED photography lights around the arena on four sides and mounted a color camera (BFS-U3-200S6C-C: 20 MP, 18 FPS, Sony IMX183, Color) to the frame with a 16mm 10MP Telephoto Lens for a Raspberry Pi HQ Camera. For experiments, behavioral trials were run for 24 hours at 5 frames per second. When beetles survived or were physically intact enough, their CHCs were extracted, along with two of each ant type from the run, in hexane including a C18 standard for 20 minutes followed by GCMS analysis of the extracts.

Cross-maze arena

To test whether beetles could survive/navigate to a new nest of ants without any dispersal cue, a variant of the above arena was constructed in a maze configuration (Figure S7A). Only the end walls connecting the flanking colony chambers to the arena were left open, forcing the beetles to traverse a distance of ~4 meters at minimum to find a group of ants at the other end of the arena. The ants were retained behind a size-selecting door that would allow the beetle to enter, but which was too small for the ants themselves to pass through. Experiments with beetles in this arena were run for 24 hours, after which the beetles removed and their CHCs were subsequently extracted for GCMS analysis (as above for the cross arena).

Blob tracking for cross-maze distance analysis

To analyze the behavioral trials in these arenas, a combination of manual annotation and machine vision methods were used. To calculate the distance the beetles moved in search of ants in the maze, a blob tracking approach was used. Using the python implementation of OpenCV, each individual replicate (right or left arena) was first cropped and de-distorted with the warp perspective method to square the image and correct for the fish-eye effect from the wide-angle lens. Frames were downsampled to 20% of their original resolution to speed the blob tracking analysis, giving final dimensions of ~500 × 500 pixels per arena. From the resulting videos, a background frame was constructed using a median filter on ~10 frames taken uniformly at times during the first ~5 hours of the video. After making the background frame, downsampled videos were looped through, background-subtracted by frame, and blobs in the frame detected, with results saved. With the outputs of the blob tracker, detections were run through SORT¹⁷¹ to generate IDs for the tracked blobs. Short, spurious trajectories where the blob tracker made non-beetle detections were also filtered out with this information. The distances each beetle traveled in the experiment during the run was summed. Trajectories were also used to locate the farthest point in the maze that the beetle reached during the trial. The location where the beetle ended the run was manually annotated. Together, these data provided the total distance traveled, how far beetles penetrated the maze, and the beetle's position at the end of the trial. The distance traveled was correlated with the CHC level from a 20-minute extraction in hexane (with C18 standard) of the beetle at the end of the trial.

Manual curation of beetle death times

For the cross arena and cross-maze arena, time to death for beetles in the experiments was manually annotated. Videos were scrubbed through to locate the last time that the beetle moved in the arena under its own volition (thereby avoiding instances when ants moved dead beetles).

QUANTIFICATION AND STATISTICAL ANALYSIS

For the confidence intervals associated with Figures 4A and 5B, statistical analyses were performed in Python with non-parametric statistical approaches. Namely, bootstrap resampling was performed on the dataset and summary statistics (median proportion groom time or exponential curve regression, respectively) were calculated for each sample. The 95% confidence intervals for the summary statistics were then calculated based on the sample values. Box and whisker plots depict every data point from the relevant dataset. Box shows the median and the 25th and 75th percentiles for these points. Lower whiskers extend down from the 25th percentile by 1.5x the interquartile range or to the smallest datapoint, whichever is larger. Upper whiskers extend from the 75th percentile upward by 1.5x the interquartile range or to the largest datapoint, whichever is smaller. NMDS and centered log ratio transformed principal component analysis were conducted in Python/R.